NACA TN 2287

NATIONAL ADVISORY COMMITTEE FOR AERONAUTICS

TECHNICAL NOTE 2287

AN INVESTIGATION OF PURE BENDING IN THE PLASTIC RANGE WHEN LOADS ARE NOT PARALLEL TO A PRINCIPAL PLANE

By Harry A. Williams

Stanford University

Washington
February 1951

NATIONAL ADVISORY COMMITTEE FOR AERONAUTICS

TECHNICAL NOTE 2287

AN INVESTIGATION OF PURE BENDING IN THE PLASTIC RANGE WHEN LOADS ARE NOT PARALLEL TO A PRINCIPAL PLANE

By Harry A. Williams

SUMMARY

Rectangular beams and I-beams of aluminum alloy 75S-0 were tested in pure bending in the plastic range with the plane of loading at angles of 0°, 30°, 60°, and 90° to the minor principal axis of the cross section. It was found that Cozzone's method of plastic bending analysis gave reasonable correlation between theoretical and experimental bending moments for the plastic range beyond the yield strength. The analysis is approximate since it assumes that the neutral axis does not rotate or translate. The latter occurs in all cases and the former occurs when the loads are not parallel to a principal plane.

Similar tests of an exploratory nature were made with angle cross section beams. A modification of Cozzone's method gave reasonable results for some positions of loading but not for others.

INTRODUCTION

Numerous solutions have been proposed for the problem of pure bending in the plastic range when the loads are parallel to a principal plane of bending. The earlier work of Saint Venant is presented in reference 1. Solutions based on an exponential relationship between stress and strain have been used by a number of investigators (references 2 to 4). Semigraphical solutions are presented in references 5 and 6.

When the problem of plastic bending arises in practice, it is usually not the simple case treated in the references. The plane of loading may not coincide with a principal plane of bending and shear or axial loading is often present. Hence, the present investigation was undertaken to determine whether a reasonably simple solution could be found for the particular problem of pure bending when the loads were not parallel to a principal plane.

This work was conducted at Stanford University under the sponsorship and with the financial assistance of the National Advisory Committee for Aeronautics.

SYMBOLS

a_c	distance to midpoint of neutral axis, inches
Δa_c	change in a_c, inches
c	one-half depth of symmetrical beam, inches
c_c, c_t	distance from neutral axis to outer compressive and tensile fibers, respectively, inches
c_N	distance from rotated neutral axis to outer fibers of symmetrical beam, inches
e	general symbol for strain, inch per inch
e_c, e_t	outer fiber compressive and tensile strain, respectively, inch per inch
e_1 to e_4	strains determined experimentally, inch per inch
f	normal stress, psi
f_p, f_y	proportional limit stress and yield strength, respectively, from average stress-strain curve, psi
f_m	outer fiber bending stress, psi
f_{mc}, f_{mt}	outer fiber compressive and tensile stress, respectively, in angle beams, psi
f_O	Cozzone's intercept stress, psi
f_{Oc}, f_{Ot}	intercept stress for compressive and tensile area, respectively, of angle beams, psi
k	Cozzone's beam section constant
k_c, k_t	beam section constant for compressive and tensile areas, respectively, of angle beams

x_b, x_u x_n, y_n	distance to point on rotated neutral axis, inches
E	Young's modulus of elasticity, psi
I_N	moment of inertia of cross section with respect to neutral axis, inches^4
I_x, I_y, I_{xy}	moment and product of inertia of cross section with respect to x- and y-axes, inches^4
I_X, I_Y	moments of inertia of angle beam cross section with respect to principal axes, inches^4
I_{Nc}, I_{Nt}	moments of inertia of compressive and tensile areas, respectively, with respect to neutral axis of angle beam cross sections, inches^4
K_f	plastic bending factor based on average stress-strain curve, psi
L	moment arm, inches
M_t	experimental bending moment, inch-pounds
M_{th}	bending moment computed analytically, inch-pound
M_{th}', M_{th}''	bending moments computed analytically for compressive and tensile areas, respectively, of angle beams, inch-pounds
Q_m	statical moment of one-half of symmetrical beam cross section, inches^3
Q_{mc}, Q_{mt}	statical moments of compressive and tensile areas, respectively, of angle beams, inches^3
W	total load on beam, pounds
β	angle between principal axis and neutral axis, degrees
$\Delta\beta$	change in angle β, minutes
θ	angle between plane of loading and y-axis, degrees
ϕ	angle between plane of loading and normal to rotated neutral axis, degrees

TEST SPECIMENS AND APPARATUS

Test specimens.- The test specimens were from a single shipment of annealed aluminum alloy 75S-O bars, which were 1 inch thick and 2 inches deep. The rectangular specimens were merely cut to length from the full bar. The I-beams and angle beams were machined to the dimensions shown in figure 1. The maximum variation from the dimensions shown in the figure was 0.005 inch. Since this variation changed the analytical results by less than 1 percent, the section properties were based on the nominal dimensions throughout this report. Photographs of typical specimens after testing are shown in figure 2.

It was decided to use the 75S-O material after investigation of other materials. It had been originally planned to use 24S-T aluminum alloy,[1] but preliminary experience indicated that there was considerable difference between the stress-strain curves in tension and compression. In order to eliminate this variable as far as possible and also obtain a material which would reach the plastic range as soon as possible, the aluminum alloys 61S-O, 61S-W,[1] and 75S-O were all sampled. In all cases the compression stress-strain curve was above the tension curve, but the 75S-O had curves which were more nearly alike. However, when the shipment arrived, samples from it showed a greater variation between the two curves.

In selecting the annealed aluminum alloy for the test specimens, it was realized that they could not be bent to rupture. This had two advantages. There would be no risk to gaging equipment as a result of such failure and the distortion of bent specimens could be studied more easily if the specimens were still in one piece.

Loading apparatus.- The arrangement of the loading apparatus used in the tests is shown in figure 3. A cross beam was mounted on top of a 20,000-pound Emery capsule which was in turn mounted on the upper or stationary head of a 200,000-pound-capacity Riehle testing machine. The capsule was supported on ball bearings and could be operated by a chain-driven screw so that the whole assembly moved laterally, thus keeping the suspender rods in a vertical plane if necessary. The loading jig in which the specimen was placed is shown in figures 4 and 5. It was mounted on the upper side of the moving head of the testing machine and, as the head was lowered, the jig applied third-point loading to the specimen. Provision was made for movement of the interior supports toward each other as the beam curvature became large by having each support mounted on ball bearings and actuated by a centering device (not shown in the figures), which maintained symmetry with respect to a center line.

[1]New temper designations for alloys given are: 24S-T4 for 24S-T and 61S-T4 for 64S-W.

It will be noted that the third-point knife-edge assembly was arranged to rotate about one axis. When the beam was to be tested at an angle to the vertical, this whole assembly was rotated and bolted in place at this angle. The construction used then allowed the beam to rotate the knife edges as it bent about the weaker axis and considerable restraint was thus eliminated. After the rectangular beams were tested, ball bearings were inserted at the knife-edge spindles in order to eliminate friction.

The fittings which connected the ends of the beam to the suspender rods are shown in figure 6. It will be noted that these fittings allowed for three degrees of freedom. The action of the loading jigs and end fittings can be seen in the photographs of figures 7, 8, and 9. The photograph of figure 10 shows the general arrangement.

Strain apparatus.- Strains were recorded automatically by the Brown strip-type potentiometer which is shown on the table at the left in figure 10. Strains were measured at the outer corners of all beams by special electrospring-type gages which can be seen in the photographs. These gages consisted of two hardened steel knife edges, 2 inches apart and connected at the top by a piece of spring steel 0.438 inch wide and 0.016 inch thick. SR-4 electric strain gages were cemented to the top and bottom sides of the spring steel. Since the resistance change was of opposite sign in the two gages, they acted together to unbalance a Wheatstone bridge and thus increase the sensitivity. The electrospring gages were mounted as shown in figure 9. Their accuracy will be discussed later in the report.

SR-4 electric strain gages cemented to the specimens were used rather sparingly and only for checking purposes in the elastic range when early experience indicated that they were liable to go out of action any time after the strain reached 1 percent. A comprehensive test in which 10 strain gages of type A-12 were used is shown in figure 9 for beam G-1, which was a rectangular beam in the 60° position.

TEST PROCEDURE

Stress-strain characteristics of material.- The 75S-0 aluminum alloy bars were shipped in 12-foot lengths. The bars used in the investigation were lettered from A to G. Six beam specimens $19\frac{1}{2}$ inches long and two 13-inch sections from which tension and compression specimens could be taken were cut from each bar. The first 13-inch section was taken 39 inches from one end of a bar and the other, $19\frac{1}{2}$ inches from the other end. Three tension specimens and two compression specimens were taken from each 13-inch section. The tension specimens were 8 inches long and were machined to 1/8 by 1/2 inch at the reduced section. One specimen was cut from the outside and the other two were cut from the interior of the bar. The compression specimens which were finally used were 15/16 inch by 1 inch by 3 inches in length and might be referred to as the block type of compression specimen.

The tension specimens were tested in the conventional manner with an Ames dial extensometer having a 2-inch gage length. The block compression specimens were carefully squared and placed in the testing machine so that the compression stress was as uniform as possible. The deformation was measured with a 1-inch gage length Ames dial extensometer. Readings were taken until the specimen had buckled considerably, which was usually when the strain had reached 8 to 10 percent.

The results of all stress-strain tests are shown in figures 11 and 12. All specimens from bars A, B, and C were tested, but, since the scatter was not large, only a few specimens from the remaining bars were tested to check the uniformity of the shipment.

A number of compression tests were made on strip specimens which were 1/8 inch by 1 inch by 2 inches. The specimens were supported laterally by two pieces of cold-rolled steel between stiff springs. The specimen was 1/8 inch shorter than the cold-rolled steel side pieces and the load was applied by means of a steel strip approximately 0.11 inch thick. Strains of the order of 6 percent could be obtained by this method before the specimen buckled. However, the stress-strain curve obtained from these tests was about 2000 psi higher than the corresponding curve obtained from the block compression tests. Since it was believed that this difference resulted from friction and lateral pressure, it was decided that the block compression specimens gave a better average value of the properties of the material. Hence, tests of the strip-type specimens were discontinued.

<u>Calibration of strain gages</u>.- The electrospring gages were mounted on the apparatus shown in figure 13 and calibrated against a 0.0001 inch Ames dial. When the Ames dial readings were plotted against divisions on the recorder chart, the relationship was very close to linear. The maximum variation in strain was 0.0005 inch per inch for range 2 of the recorder (11 in. on the chart equals 10-percent strain) and was about the same for range 3 (11 in. on the chart equals 5-percent strain). The recorder chart contained 200 divisions in the 11-inch width. Readings were estimated to the nearest tenth of a division.

The gages were calibrated seven different times during the course of the tests. The maximum variation from the average of all calibrations for any one gage was 3.5 percent.

Tests of beams.- Each beam specimen was scribed and measured with a micrometer to the nearest 0.001 inch and placed in the loading jig with the third-point supports set at the desired degree of rotation. The third-point loading was used in all but a few cases in which the moment arm L (fig. 1) was 9 inches instead of 8 inches. When the angle θ was 30° or 60°, the beam had a tendency to rotate about a longitudinal axis. This was prevented by wedging the beam in the interior supports. Under these conditions, restraint at the interior supports was largely eliminated by the rotation of the knife-edge assembly. There was, however, always an indeterminate amount of restraint against bending with respect to the x-axis of the beam.

The electrospring gages were attached to the corners of the beam as shown in figure 9. The knife edges were set on previously scribed lines approximately 2 inches apart. The gages were set at zero on the recorder chart after a small initial load had been applied to the beam, and an additional load was usually applied and removed to check the recorder.

The normal testing procedure was to apply an increment of load, stop the testing machine, and immediately start the recorder. The latter step was particularly important in the plastic range because of creep.

As the plastic range was reached, the curvature of the specimen decreased both the distance between the suspender rods and the distance between the interior load points. Changes in the latter were measured to the nearest 0.01 inch by means of the Ames dial shown at the lower left in figure 8. The changes in the suspender-rod distance were measured to the nearest 0.01 inch by means of the longitudinal scale shown in the same figure. The change in the length of the moment arm L was computed from these values.

The moving head of the testing machine was operated at a speed of 0.1 inch per minute until the strain was of the order of 0.0250 inch per inch, after which the speed was changed to 0.4 inch per minute.

Specimens were removed when the strain was between 4 and 10 percent in the outer fiber, depending on the depth of the beam. Tests were usually continued until the curvature was so great that the interior knife edges were in danger of slipping toward the center or until other parts of the apparatus threatened to interfere with the normal action of the jig.

When the angle θ was 30° or 60° for the symmetrical beams and at all angles for the angle cross section beams, the outer ends of the specimens moved laterally as much as 2 inches. However, the suspender rods were kept in a nearly vertical plane by operating the pull chain from time to time, thus moving the capsule assembly laterally.

In the case of the angle beams, the rotation of one leg was measured by clamping an arm to the longer leg. A protractor and plumb bob at the end of this arm enabled the rotation between the interior load points to be read to the nearest 0.2°.

ANALYTICAL PROCEDURE

When the loads are not parallel to a principal plane and the outer fiber stresses are in the plastic range, it is obvious that the principal of superposition ordinarily used in the elastic range is no longer suitable. However, the problem can be solved by treating it as one in pure bending with respect to the true neutral axis. This is an alternative solution in the elastic range, also, and is illustrated in a number of textbooks on elementary strength of materials.

The approach to the problem was to determine the location of the neutral axis in accordance with the conventional methods used for the elastic condition. The bending moment with respect to this neutral axis is equal to the cosine component of the resultant bending moment. It was recognized that, if the neutral axis translated or rotated as the plastic range was reached, it would be necessary to make a new solution for every value of the bending moment. However, it was determined during the investigation that large errors were not introduced by neglecting this factor and the solution in the plastic range could be based on the assumption that the neutral axis remained stationary.

Several methods of relating stress to bending moment with respect to the neutral axis were investigated. The use of a plastic bending factor (reference 6) was discarded because a solution by this method would require a large amount of tedious computation since the method is primarily applicable to rectangular cross sections which are perpendicular to the neutral axis.

A solution based on an exponential relationship between stress and strain was next investigated. It was found that when the product fe was plotted on logarithmic paper against the strain e, a straight-line relationship was obtained for that portion of the stress-strain curve beyond the yield strength. This relationship could be expressed in the form $fe = ae^n$. However, the expression for bending moment contained the quantity $\int y^n \, dA$ instead of the usual term for moment of inertia. This led to a simple approximate solution for the rectangular beams when the plane of loading coincided with a principal axis, but otherwise the approximate result obtained hardly justified the labor involved.

Further investigation indicated that the method presented by Cozzone (reference 5) offered the best possibility for a solution which would be reasonably simple to apply, although the result would be approximate. Cozzone's expression was

$$M_{th} = \frac{I_N}{c}\left[f_m + f_0(k - 1)\right] \tag{1}$$

where $k = \dfrac{2Q_m}{I_N/c}$. The intercept stress f_0 is related to the plastic bending factor K_f (reference 6) as follows:

$$f_0 = 6K_f - 2f_m \tag{2}$$

As presented by Cozzone in reference 5, the method is based on the assumption that the stress-strain curve for tension is identical with that for compression and the neutral axis is an axis of symmetry. Actually, equation (1) is approximate for any cross section which is not rectangular even when the stress-strain curves are identical (see under "Discussion," reference 6). Since in the plastic range the stress-strain curves in tension and compression are not identical for most materials and the neutral axis must continually change position accordingly, equation (1) results in an approximate solution even for a rectangular cross section. However, the method gives reasonable results because of compensating errors and because in the plastic range the restraining moment is not sensitive to even large errors in strain.

When the beam cross section is symmetrical but the plane of loading does not coincide with a principal plane of bending (figs. 14 and 15), equation (1) becomes

$$M_{th} = \frac{I_N}{c_N}\frac{1}{\cos \phi}\left[f_m + f_0(k - 1)\right] \tag{3}$$

It is apparent from figures 14 and 15 that the neutral axis is not an axis of symmetry. However, the tension and compression areas of these beams contribute equally to the restraining moment with respect to the neutral axis as long as stress-strain curves in tension and compression are identical. This further implies that the neutral axis does not translate or rotate from its elastic-range position.

It might be noted that, if the exact location of the neutral axis is known, it is possible to modify equation (3) to obtain a more accurate solution. However, a designer would find the computation required for this determination extremely tedious. It would be highly impractical to locate the neutral axis by analytical methods.

Equation (3) can be modified for an unsymmetrical cross section such as the angle beam of figure 16(a). Additional errors are introduced by the rotation of the beam in the plastic range. Neglecting this factor, a rough solution may be made by dividing the cross section into a compression area and a tension area. The resisting moment of the compression area is obtained by assuming the symmetrical cross section shown in figure 16(b). The resisting moment of this beam is computed and divided by two. This is equivalent to computing I_{Nc} for one-half the cross section only. Then $k_c = \frac{2Q_{mc}}{2I_{Nc}/c_c} = \frac{Q_{mc}}{I_{Nc}/c_c}$ and the moment becomes

$$M_{th}' = \frac{I_{Nc}}{c_c} \frac{1}{\cos \phi}\left[f_{mc} + f_{0c}\left(k_c - 1\right)\right] \qquad (4)$$

A similar approach for the tension area (fig. 16(c)) results in the equation:

$$M_{th}'' = \frac{I_{Nt}}{c_t} \frac{1}{\cos \phi}\left[f_{mt} + f_{0t}\left(k_t - 1\right)\right] \qquad (5)$$

The final restraining moment is

$$M_{th} = M_{th}' + M_{th}'' \qquad (6)$$

Further investigation may develop a simpler solution.

It is easier to compare experimental and theoretical bending moments in the plastic range than to compare outer fiber stresses; hence, the general procedure used in this investigation has been to take the experimental strain corresponding to a given load, determine the necessary stress values from a representative stress-strain curve, and then insert these in the appropriate formula to compute the so-called "theoretical bending moment."

In order to check the experimental procedure as a whole, the shifting of the neutral axis was taken into account when computing the theoretical bending moments by the method of reference 6 for the rectangular beams in the 0° and 90° positions. Since it was deemed impractical to take into account the shift and rotation of the neutral axis for the other cases, in which Cozzone's solution was used, it was necessary to decide whether the computations should be based on the tension curve only, as proposed by Cozzone, or on an average of the tension and compression curves. It was reasoned that if an average curve gave acceptable results, it would be safest to use this approach for materials having decidedly different properties in tension and compression. It was apparent that solutions based on the tension curve could give satisfactory results only because of compensating errors. (Some comparisons between the two approaches are made later in the report.) Hence, the curves of figures 17 and 18 were constructed on this basis. Strains were plotted to an enlarged scale in figure 17 to facilitate reading of values when strains were small.

The curves of figures 17 and 18 were constructed originally from the coupon results for bars A and B. It was found, however, that results would be affected only about 1.5 percent if the same curves were used for all bars.

RESULTS AND DISCUSSION

Strain measurements.- Typical load and strain data are recorded in tables 1 to 3. The total load registered by the weighing apparatus is given in the first column. The moment arm is given in the second column, and it will be noted that it decreases as the curvature of the beam becomes larger. The experimental bending moment is the product of the moment arm times one-half the total load. The measured strains have been computed by multiplying the number of divisions on the recorder chart by the appropriate calibration factor.

The electrospring strain gages were designed to measure large strains and as a result could not be relied upon to give suitable accuracy in the elastic range. This deficiency was partially overcome by plotting strain readings for each gage against the experimental bending moment. Selected results are shown for each group of tests in figures 19 to 22. The procedure adopted was to use the values from a straight line which was representative of the plotted points if the resulting computed moments were within about 10 percent of the experimental moment. If the discrepancy was larger, it was assumed that the gages had not operated correctly and a line having approximately the correct theoretical slope was substituted. An average value of $E = 10.25 \times 10^6$ psi was used in computing the theoretical slope.

The justification for this procedure is that the investigation was primarily concerned with the plastic range beyond the yield strength of the material. A difference of even 0.0010 inch per inch in the strain had negligible effect on the results in this range. Results for that portion of the range between the proportional limit and the yield strength were usually changed 2 to 5 percent by the procedure. However, no great accuracy can be expected in this range as long as the computation is based on an average stress-strain curve.

The corrected strains given in tables 1 to 3 were obtained from curves of M_t against e such as those in figures 19 to 22. These strains were recorded to the nearest tenth of a ten-thousandth when read from the curves. When they were recorded to two figures to the right of the decimal point for the elastic range, the values were computed by formula. The figure beyond the decimal point was dropped arbitrarily when the strain reached 100×10^{-4} inch per inch in the interests of consistency. Obviously, such figures ceased to have significance long before.

Strain readings were of the same order of magnitude in general for the specimens of the same group. The main exceptions to this were usually near the end of an experiment when the curvature had become quite large. The discrepancy was probably due to some extent to an inability to duplicate exactly conditions in each test. In the plastic range, relatively small differences in loading conditions may result in large changes in outer fiber strain. The strain gages were a factor also because it was found that certain gages sometimes became unstable when the curvature became large. The gages were attached in pairs and, if the spring tensions were higher on one side of the beam than on the other, the pair of gages occasionally rotated slightly. The test was always continued with them in this position since it was believed that the error would be more serious if the gages were readjusted to their original position. Such discrepancies did not greatly affect the computed bending moment because even large changes in outer fiber strain did not affect the stress factors after the stress-strain curves had flattened out.

The strain gages obviously measured the change in length of the chord distance between the knife edges. When the strain was 10 percent for a 2-inch-deep beam or 5 percent for a 1-inch-deep beam, the discrepancy amounted to about 0.0015 inch per inch. This amount should be added to the tension strain and subtracted from the compression strain. Since such discrepancies would have a negligible effect on the computed bending moment when the strains were of this order of magnitude, this factor was neglected.

Theoretical and experimental bending moments.- The correlation between the theoretical and experimental bending moments is shown graphically in figures 23 to 25. The differences are computed from the expression $\left(\frac{M_{th}}{M_t} - 1\right) \times 100$ percent. The elastic, semielastic, and plastic ranges are shown in these graphs by indicating on the moment scale the approximate values of the experimental moment at which the proportional limit f_p and the 0.2-percent offset yield stress f_y were reached in the outer fibers of the beam in question.

The theoretical bending moments were computed as shown in tables 4 to 6. The quantities in the formulas which depend upon section properties are given in figures 14 to 16.

An inspection of figures 23 to 25 shows that the theoretical bending moment was within 10 percent of the experimental moment in the plastic range beyond the yield strength and was usually within 15 percent between the proportional limit and the yield strength. Some of the angle beams and one group of I-beams ($\theta = 30^\circ$), where twist was involved, were exceptions to this statement.

The twist mentioned above results from the fact that, when the beam curvature is not in the same plane as the applied moment couple $\frac{W}{2}L$, this couple can be resolved into components concerned with bending and a torsion component at any point on the curved beam. The torsion is maximum at the support and decreases to zero at the center. When the maximum moment of inertia of a beam cross section is large compared with the minimum value and the torsional rigidity is small, the torsion component becomes an important factor in the failure of some beams through loss of stability.

The beams used in this investigation, with the exception of one rectangular beam, failed by excessive twisting when the angle θ was 30°. It is quite probable that the beams in the 0° position did not fail in the same way because the tests could not be carried far enough. This conclusion is consistent with the known behavior of deep, narrow beams. Had longer spans been used in the investigation, torsional instability would have been more prominent.

Alternate method of computing moments.- The theoretical bending moments were computed for the rectangular beams and the I-beams on the basis that the outer fiber strain was an average of the maximum tensile and compressive strain. However, some comparisons were made on the assumption that the outer fiber tensile strain governed and that the compression stress-strain curve was identical with the tension curve, in accordance with Cozzone's original proposal. It developed that the computed bending moment was between 5 and 10 percent higher for that region where the tensile stress-strain curve is above the compression curve. Through the middle region where the curves crossed there was little to choose between the two methods. In the later stages of plastic bending, the tension curve resulted in moments which were between 2 and 5 percent lower. Hence, it would be more conservative for the designer to use the average curve in the earlier stages of plastic bending and the tension curve in the later stages. Obviously, the percentages given above apply only to the particular material used in this investigation.

Deflections.- No particular attempt was made to measure the deflections of the beams tested, although some approximate observations were taken. However, it is obvious from the photographs of tested specimens (fig. 2) that the final deflections were large. Deflection rather than resistance to plastic bending may govern many designs.

Change in position of neutral axis.- Dimensions from which the neutral axis could be located (see figs. 14 to 16) were computed for all beams. Sample results are shown in the second and third columns of tables 4 to 6, primarily as a matter of interest. The distances were computed from the appropriate corrected strains by simple proportion. The results are rough approximations only, because these distances are quite sensitive to small changes in strain. When a gage was near the neutral axis and the strains were relatively small, the effect of errors in the strain was quite pronounced. However, the results for a given group of tests indicated trends when considered collectively. Dimensions are given in the tables to 0.001 inch merely to indicate the trend when variations are small.

Inspection of the values of c_c and c_t for the symmetrical beams in the 0° and 90° positions (figs. 14 and 15) showed that the neutral axis moved toward the tension side of the beam as the stress exceeded the proportional limit. This trend continued until the yield strength had been passed, when the trend was reversed and the movement was toward the compression side. Theoretically, this was to be expected. When the compression stress-strain curve was below the tension curve, the neutral axis had to move down and put more of the beam cross section in compression in order that the total compressive force on one side of the axis would balance the total tensile force on the other side.

The sample curves in figure 26 show the rotation and translation of the neutral axis for two of the rectangular beams in the 30° position. The lack of symmetry in this case results in both a rotation and a translation to balance the compressive and tensile forces on the cross section. The change in angle β for the symmetrical beams (figs. 14 and 15) may be computed from the expression

$$\Delta\beta = (90^\circ - \beta) - \tan^{-1} \frac{x_b + x_u - 1}{2} \tag{7}$$

The change in the midpoint distance a_c is equal to

$$\Delta a_c = \frac{x_b - x_u}{2} \tag{8}$$

These expressions are derived from simple geometrical relationships.

The 60° rectangular beams followed the trend indicated in figure 26. The maximum clockwise rotation was of the order of 2°, and the curve did not recross the axis. The maximum decrease in a_c was about 0.03 inch, and the maximum increase was of the order of 0.02 inch. The I-beams at 30° and 60° followed much the same pattern, and the magnitudes were of the same general order.

The unsymmetrical angle beams rotated and translated for all load positions. The geometry of figure 16 gives the following expressions for the changes:

$$\Delta\beta = (90^\circ - \beta) - \tan^{-1} \frac{x_n}{y_n} \tag{9}$$

$$\Delta a_c = 0.261 - 0.760 \frac{x_n}{y_n} + x_n \tag{10}$$

In general, rotations were all clockwise. The order of magnitude was about 1° for the 0° position, 2° for the 30° position, and 3° for the 60° and 90° positions. The distance a_c increased about 0.07 inch for the 0° position but showed little change for the 30° position. It increased 0.01 inch and 0.03 inch in the 60° and 90° positions, respectively.

Rotation of angle beams.- The rotation of the 2-inch leg of most of the angle beams was measured. Typical results are shown in table 6.

The rotation was clockwise (see fig. 16), and the maximum values were of the following order of magnitude:

Angle θ (deg)	Rotation (deg)
0	3
30	7
60	2.5
90	.2

Good correlation between theoretical and experimental bending moment was consistent with small rotation.

APPLICATION OF RESULTS TO PRACTICAL DESIGN

So far, plastic bending analysis has been applied primarily to cast and forged materials. Other applications may be found as plastic bending theory is extended. This investigation is considered as a step in that direction.

The question might be raised as to whether results obtained for a soft material such as aluminum alloy 75S-O are applicable to the same materials in the hardened state and to cast materials. The question applies particularly to predicting the ultimate bending strength. There is no reason to believe that the approach suggested in this report will not apply to such materials. A limited number of tests to failure have been made on 24S-T rectangular and I-beams when the loads were in a principal plane of bending (reference 6). When the loads are not in a principal plane of bending, the neutral axis does not coincide with a principal axis, but otherwise the general behavior is approximately the same. The experiments reported in this investigation were continued until the stress-strain curves had flattened out and there was little change in bending moment with increase of curvature. This condition will prevail until the beam ruptures, local crippling occurs, or deflection becomes excessive.

CONCLUSIONS

The following conclusions may be made from the results of the investigation as far as symmetrical cross section beams are concerned:

1. A modification of Cozzone's method of handling plastic bending problems gives approximate but reasonable results when the plane of loading does not coincide with a principal axis. For the particular material investigated, the correlation between computed and experimental bending moments in the plastic range beyond the yield strength was within 10 percent for all but a few beams. The correlation will vary for other materials, depending on the uniformity of the material and the relationship between the tension and compression stress-strain curves.

2. If the properties of the material are similar to those of the material used in the investigation and the computed bending moment is based on the tensile stress-strain curve rather than on a curve which is an average of the tensile and compressive curves, the results will be less conservative in the region of the yield strength and more conservative in the later stages.

3. If the flanges become unstable and buckle along the edges in the plastic range, the computed moments will be on the unconservative side.

4. This investigation has been restricted to relatively short span beams. Most of the beams tested in the 30° position failed from excessive twisting. This type of failure will be more pronounced as the span length is increased.

5. No generalizations can be made from the results of the exploratory tests of angle cross section beams because the results may be quite different for cross sections of different proportions from those used in the investigation.

Stanford University
Stanford University, Calif., December 16, 1947

REFERENCES

1. Timoshenko, S.: Strength of Materials. Part II - Advanced Theory and Problems. Second ed., D. Van Nostrand Co., Inc., 1941.

2. Beilschmidt, J. L.: The Stresses Developed in Sections Subjected to Bending Moment. Jour. R.A.S., vol XLVI, no. 379, July, 1942, pp. 161-182.

3. Osgood, William R.: Plastic Bending. Jour. Aero. Sci. vol. 11, no. 3, July 1944, pp. 213-226.

4. Rappleyea, F. A., and Eastman, E. J.: Flexural Strength in the Plastic Range of Rectangular Magnesium Extrusions. Jour. Aero. Sci., vol. 11, no. 4, Oct. 1944, pp. 373-377.

5. Cozzone, Frank P.: Bending Strength in the Plastic Range. Jour. Aero. Sci., vol. 10, no. 5, May 1943, pp. 137-151.

6. Williams, Harry A.: Pure Bending in the Plastic Range. Jour. Aero. Sci., vol. 14, no. 8, Aug. 1947, pp. 457-469.

TABLE 1.- LOAD AND STRAIN DATA FOR RECTANGULAR BEAM A-6 WHEN $\theta = 30^{\circ}$

Total load, W (kips)	Moment arm, L (in.)	Experimental bending moment, M_t (in.-kips)	Measured strains (in./in.) (a)				Corrected strains (in./in.) (a)(b)			
			e_1 (-)	e_3 (+)	e_2 (+)	e_4 (-)	e_1 (-)	e_3 (+)	e_2 (+)	e_4 (-)
0	8.00	0	----------	----------	----------	----------	0	0	0	0
.15	8.00	.60	0	0	0	0	$.1 \times 10^{-4}$	1.7×10^{-4}	$.1 \times 10^{-4}$	1.6×10^{-4}
.25	8.00	1.00	$-.5 \times 10^{-4}$	2.0×10^{-4}	$.9 \times 10^{-4}$	1.6×10^{-4}	.2	2.8	.1	2.8
.50	8.00	2.00	-.7	5.5	-.4	4.1	.6	5.3	.2	5.5
.76	7.99	3.04	-.7	8.3	-.4	6.8	.8	8.3	.4	8.1
1.00	7.98	3.99	0	9.8	-.4	10.1	1.0	11.0	.7	11.0
1.25	7.98	4.99	.2	12.6	-.4	12.2	1.1	13.8	.8	13.5
1.50	7.97	5.98	.2	15.6	.4	15.7	1.3	16.2	.9	16.5
1.77	7.97	7.05	-.5	18.9	.7	19.6	1.5	19.0	1.0	20.0
2.00	7.97	7.97	.5	21.4	.9	22.2	1.7	21.8	1.1	23.0
2.25	7.96	8.96	.5	24.7	.4	25.3	1.9	24.7	1.3	26.0
2.50	7.95	9.94	.5	28.5	.4	30.1	2.0	28.5	1.5	30.5
2.75	7.94	10.91	1.7	32.5	.9	34.6	2.1	32.5	1.7	35.5
3.00	7.93	11.90	2.9	37.5	.9	40.2	2.9	37.5	1.9	41.5
3.26	7.92	12.91	2.9	43.5	2.0	48.0	3.9	43.5	2.0	49.5
3.50	7.91	13.84	4.2	51.5	1.1	57.2	4.9	51.5	2.1	58.5
3.75	7.90	14.80	5.4	62.2	2.0	70.0	6.2	62.5	2.6	71.5
4.00	7.89	15.80	6.2	78.0	2.8	87.7	8.0	78.0	3.5	89.5
4.50	7.87	17.70	10.6	130	4.4	143	11.5	130	5.5	144
5.00	7.80	19.50	15.3	214	7.7	230	16.0	214	8.5	231
5.50	7.68	21.10	20.2	337	18.9	357	21.5	337	19.5	358
6.00	7.52	22.60	29.1	496	40.7	542	32.0	496	42.0	543
6.25	7.41	23.20	37.5	599	62.9	660	37.5	599	56.0	661
6.50	7.34	23.80	49.9	695	84.5	773	47.0	695	76.0	774
6.75	7.28	24.60	58.4	809	103	902	53.0	809	110	903

[a]Tension, +; compression, -.
[b]Corrected from curves of M_t against e. In elastic range, slopes made to agree approximately with theoretical slopes.

TABLE 2.- LOAD AND STRAIN DATA FOR I-BEAM C-5 WHEN $\theta = 30^{\circ}$

Total load, W (kips)	Moment arm, L (in.)	Experimental bending moment, M_t (in.-kips)	Measured strains (in./in.) (a)				Corrected strains (in./in.) (a)(b)			
			e_1 (-)	e_3 (+)	e_2 (-)	e_4 (+)	e_1 (-)	e_3 (+)	e_2 (-)	e_4 (+)
0	8.00	0	------------	------------	------------	------------	0	0	0	0
.05	8.00	.20	0	0	0	0	$.52 \times 10^{-4}$	1.49×10^{-4}	1.49×10^{-4}	$.52 \times 10^{-4}$
.08	8.00	.30	$.2 \times 10^{-4}$	$.8 \times 10^{-4}$	1.9×10^{-4}	$.2 \times 10^{-4}$	.78	2.23	2.23	.78
.10	8.00	.40	.5	1.0	2.1	.4	1.05	2.97	2.97	1.05
.15	8.00	.60	2.4	2.3	3.1	.8	1.57	4.46	4.46	1.57
.20	8.00	.80	1.0	4.9	4.2	.8	2.09	5.94	5.94	2.09
.25	7.99	1.00	1.9	5.4	6.5	1.0	2.62	7.43	7.43	2.62
.30	7.99	1.20	2.9	6.5	7.7	2.1	3.14	8.92	8.92	3.14
.35	7.99	1.40	3.1	8.3	9.0	2.3	3.66	10.40	10.40	3.66
.40	7.99	1.60	4.3	9.8	11.3	3.6	4.18	11.89	11.89	4.18
.46	7.99	1.84	4.3	10.9	13.0	4.0	4.6	13.5	13.3	4.7
.50	7.99	2.00	5.1	12.4	14.2	4.4	5.2	14.0	14.8	5.2
.55	7.99	2.20	5.3	14.0	16.7	4.9	5.8	14.7	16.4	5.9
.60	7.99	2.40	5.1	17.0	18.2	5.7	6.4	17.0	18.2	6.6
.65	7.99	2.60	7.5	15.5	20.9	7.2	7.2	18.4	20.1	7.3
.70	7.99	2.80	8.2	17.3	22.4	8.2	7.8	19.9	22.2	7.9
.75	7.99	3.00	9.6	18.1	25.5	8.9	8.7	21.2	24.4	8.6
.80	7.99	3.20	8.4	21.2	27.0	9.5	9.9	22.5	26.8	9.7
.90	7.99	3.60	12.3	23.3	30.9	12.2	12.2	26.8	32.2	12.3
1.00	7.99	3.99	14.9	31.0	39.7	14.6	14.7	32.5	39.0	15.2
1.10	7.98	4.38	19.5	39.8	46.4	18.6	18.0	41.8	47.5	19.6
1.20	7.98	4.78	22.2	48.6	57.2	24.9	22.2	50.6	59.0	25.5
1.30	7.98	5.18	27.7	63.3	73.0	34.2	27.5	63.5	73.0	32.5
1.40	7.97	5.67	36.6	80.5	97.5	43.7	36.6	82.5	97.5	44.2
1.50	7.96	5.97	46.9	94.0	116	54.7	46.0	96.0	116	55.2
1.60	7.94	6.36	65.0	133	166	75.0	65.0	135	166	75.5
1.65	7.92	6.53	75.1	152	195	88.0	75.1	154	195	88.5
[c]1.70	7.90	6.72	79.4	162	211	95.0	79.4	164	211	95.5
1.75	7.88	6.90	101	204	258	122	101	206	248	122
1.80	7.83	7.04	107	254	308	155	107	256	308	156
1.85	7.80	7.22	124	385	330	162	124	387	330	162
1.90	7.68	7.30	174	465	413	229	174	467	413	230
1.95	7.51	7.32	215	535	541	314	215	537	541	314

[a]Tension, +; compression, -.
[b]From curves of M_t against e. In elastic range, slopes made to agree with theoretical slopes.
[c]Evidence of outer edge of flange buckling parallel to y-axis.

TABLE 3.- LOAD AND STRAIN DATA FOR ANGLE BEAM F-2 WHEN $\theta = 60^{\circ}$

Total load, W (kips)	Moment arm, L (in.)	Experimental bending moment, M_t (in.-kips)	Measured strains (in./in.) (a)			Corrected strains (in./in.) (a)(b)		
			e_2 (-)	e_3 (+)	e_4 (+)	e_2 (-)	e_3 (+)	e_4 (+)
0	8.00	0	------------	------------	------------	0	0	0
.050	8.00	.20	0	0	0	2.75×10^{-4}	$.55 \times 10^{-4}$	3.02×10^{-4}
.075	8.00	.30	1.1×10^{-4}	0	1.8×10^{-4}	4.13	.83	4.52
.100	8.00	.40	2.6	0	2.9	5.50	1.11	6.02
.125	8.00	.50	4.3	0	4.5	6.88	1.38	7.53
.150	8.00	.60	5.8	1.0×10^{-4}	6.1	8.26	1.66	9.03
.175	8.00	.70	6.0	1.0	7.9	9.63	1.94	10.53
.200	8.00	.80	6.4	1.0	9.4	11.00	2.22	12.04
.225	7.99	.90	8.6	1.3	11.5	12.38	2.49	13.55
.250	7.99	1.00	10.5	1.8	13.5	13.76	2.77	15.06
.275	7.99	1.10	11.4	1.8	14.4	15.13	3.05	17.10
.300	7.99	1.20	13.1	2.3	16.4	16.51	3.32	18.9
.325	7.98	1.30	15.0	2.5	18.0	17.9	3.6	20.7
.350	7.98	1.40	16.7	2.5	20.3	19.5	3.9	22.7
.375	7.97	1.49	18.8	2.8	22.5	21.1	4.1	24.6
.400	7.97	1.59	20.8	3.3	24.5	23.6	4.4	27.0
.425	7.96	1.69	23.4	3.8	27.0	26.0	4.7	29.5
.450	7.96	1.79	25.3	4.3	29.2	28.6	5.0	32.6
.475	7.95	1.89	28.9	4.5	33.7	31.3	5.2	36.2
.500	7.95	1.99	32.8	4.8	38.2	34.5	5.5	40.0
.550	7.95	2.19	40.7	5.0	47.9	43.7	6.1	52.4
.600	7.94	2.38	52.9	5.3	63.8	55.9	6.6	66.3
.650	7.92	2.58	69.7	5.5	87.9	72.7	7.1	90.4
.700	7.89	2.76	91.6	5.8	119	94.6	7.6	121
.750	7.83	2.94	120	6.3	160	123	8.1	162
.800	7.78	3.12	158	7.5	218	161	8.9	220
.850	7.66	3.26	196	9.8	274	199	10.5	276
.900	7.52	3.38	245	12.3	345	248	12.8	347
.950	7.32	3.48	308	13.5	440	311	15.0	442
1.000	7.14	3.57	364	17.0	524	367	18.0	526

[a]Tension, +; compression, -.
[b]From curves of M_t against e. In elastic range, slopes made to agree approximately with theoretical slopes.

TABLE 4.- THEORETICAL BENDING MOMENT FOR RECTANGULAR BEAM A-6 WHEN θ = 30°

Experimental bending moment, M_t (in.-kips)	Neutral-axis location (in.) (a)		Average outer fiber strain, $\frac{e_3 + e_4}{2}$ (in./in.)	Average outer fiber stress, f_m (ksi) (b)	Cozzone's intercept stress, f_0 (ksi)	Theoretical bending moment, M_{th} (in.-kips) (c)	Ratio M_{th}/M_t	Difference (percent)
	x_b	x_u						
0	0.933	0.933	0	0	0	0	----	--
1.00	.935	.965	2.8×10^{-4}	2.87	0	1.02	1.02	2
2.00	.900	.965	5.4	5.54	0	1.96	.98	-2
3.04	.912	.958	8.2	8.41	0	2.98	.98	-2
3.99	.917	.942	11.0	11.28	0	3.99	1.00	0
4.99	.926	.945	13.6	13.8	.2	4.96	.99	-1
5.98	.926	.948	16.4	15.9	1.2	6.05	1.01	1
7.05	.926	.955	19.5	18.0	2.7	7.20	1.02	2
7.97	.927	.955	22.4	19.8	4.5	8.60	1.08	8
8.96	.930	.954	25.4	21.1	6.2	9.56	1.07	7
9.94	.935	.955	29.5	22.1	8.0	10.65	1.07	7
10.91	.940	.955	34.0	22.8	9.6	11.47	1.05	5
11.90	.930	.956	39.5	23.7	12.0	12.64	1.06	6
12.91	.920	.960	46.5	24.4	14.1	13.62	1.06	6
13.84	.914	.965	55.0	25.0	16.4	14.65	1.06	6
14.80	.910	.964	67.0	25.8	17.7	15.40	1.04	4
15.80	.907	.963	83.8	26.7	19.9	16.50	1.04	4
17.70	.920	.964	137	29.1	21.7	17.98	1.02	2
19.50	.932	.964	222	32.0	24.0	19.82	1.02	2
21.10	.940	.956	348	34.5	26.5	21.59	1.02	2
22.60	.940	.930	520	36.7	28.7	23.13	1.02	2
23.20	.941	.923	631	37.7	30.0	23.95	1.03	3
23.80	.938	.910	734	38.5	29.5	24.08	1.01	1
24.60	.938	.891	856	39.1	31.6	25.04	1.02	2

[a]Computed from corrected strains. These data not used in computing M_{th}.
[b]From average stress-strain curve.

$$^{c}M_{th} = \frac{I_N}{c_N} \frac{1}{\cos \phi}\left[f_m + f_0(k - 1)\right]$$

$$= 0.354(f_m + f_0)$$

TABLE 5.- THEORETICAL BENDING MOMENT FOR I-BEAM C-5 WHEN $\theta = 30^{\circ}$

Experimental bending moment, M_t (in.-kips)	Neutral-axis location (in.) (a)		Average outer fiber strain, $\frac{e_2 + e_3}{2}$ (in./in.)	Average outer fiber stress, f_m (ksi) (b)	Cozzone's intercept stress, f_0 (ksi) (b)	Theoretical bending moment, M_{th} (in.-kips) (c)	Ratio M_{th}/M_t	Difference (percent)
	x_b	x_u						
0	0.666	0.666	0	0	0	0	----	--
.80	.740	.740	5.94×10^{-4}	6.04	0	.79	0.99	-1
1.00	.730	.730	7.43	7.61	0	1.00	1.00	0
1.20	.744	.744	8.92	9.15	0	1.20	1.00	0
1.40	.740	.740	10.40	10.67	0	1.40	1.00	0
1.60	.740	.740	11.89	12.20	0	1.60	1.00	0
1.84	.747	.753	13.4	13.6	.2	1.81	.99	-1
2.00	.729	.739	14.4	14.4	.5	1.96	.98	-2
2.20	.730	.737	16.0	15.6	1.0	2.18	.99	-1
2.40	.723	.735	17.6	16.7	1.7	2.42	1.01	1
2.80	.718	.737	21.6	19.3	3.9	3.04	1.08	8
3.20	.694	.718	24.2	20.7	5.6	3.45	1.08	8
3.99	.688	.705	35.8	23.1	10.4	4.40	1.10	10
4.78	.696	.693	54.8	25.0	16.0	5.38	1.12	12
5.67	.693	.683	90.0	27.0	20.3	6.21	1.09	9
6.36	.676	.668	150	29.6	22.0	6.78	1.06	6
[d]6.72	.674	.687	188	31.0	23.2	7.11	1.06	6
7.05	.703	.663	282	33.3	25.3	7.69	1.09	9
7.22	.756	.714	358	34.7	26.7	8.05	1.11	11
7.30	.728	.679	440	35.8	27.9	8.36	1.14	14
7.32	.713	.632	539	36.8	29.0	8.65	1.18	18

[a]These values not used in computing M_{th}.

[b]Based on average strain and average stress-strain curve.

[c]Cozzone's approximate solution assuming symmetry with respect to elastic neutral axis:

$$M_{th} = \frac{1}{\cos \phi} \frac{I_N}{c_N}\left[f_m + f_0(k - 1)\right]$$

$$= 0.1312\left(f_m + f_0\right)$$

[d]Evidence of outer edge of flange buckling parallel to y-axis.

TABLE 6.- THEORETICAL BENDING MOMENT FOR ANGLE BEAM F-2 WHEN $\theta = 60^\circ$

Experimental bending moment, M_t (in.-kips)	Neutral-axis location (in.) (a)		Rotation of 2-in. leg (deg) (b)	Outer fiber strain (in./in.) (c)		Compression area (d)			Tension area (d)			Theoretical bending moment, M_{th} (in.-kips) (d)	Ratio M_{th}/M_t	Difference (percent)
	x_n	y_n		e_c	e_t	f_{mc} (ksi)	f_{0c} (ksi)	M_{th}' (in.-kips)	f_{mt} (ksi)	f_{0t} (ksi)	M_{th}'' (in.-kips)			
0	0.476	1.686	0	0	0	0	0	0	0	0	0	0	----	-
.40	.478	1.664	0	5.50×10^{-4}	6.86×10^{-4}	5.64	0	.18	7.04	0	.22	.40	1.00	0
.60	.478	1.664	0	8.26	10.28	8.48	0	.27	10.54	0	.34	.61	1.01	1
.80	.478	1.662	0	11.00	13.70	11.27	0	.36	13.8	0	.44	.80	1.00	0
1.00	.478	1.664	0	13.76	17.16	13.8	.2	.44	16.4	1.5	.56	1.00	1.00	0
1.40	.462	1.665	0	19.5	25.8	18.0	2.7	.64	21.1	6.2	.84	1.48	1.06	6
1.49	.461	1.673	0	21.1	28.0	19.0	3.6	.70	21.7	7.3	.89	1.59	1.07	7
1.59	.466	1.685	0	23.6	31.4	20.4	5.2	.78	22.5	8.8	.95	1.73	1.09	9
1.79	.467	1.700	0	28.6	37.1	21.9	7.5	.89	23.3	11.0	1.04	1.93	1.08	8
1.99	.463	1.725	0	34.5	45.6	23.0	10.1	1.00	24.3	13.9	1.15	2.15	1.08	8
2.19	.455	1.750	0	43.7	59.7	24.1	13.3	1.12	25.4	16.9	1.26	2.38	1.09	9
2.38	.458	1.788	.1	55.9	75.5	25.1	16.2	1.23	26.3	18.6	1.34	2.57	1.08	8
2.58	.446	1.822	.1	72.7	103	26.2	18.3	1.32	27.8	20.8	1.44	2.76	1.07	7
2.76	.440	1.852	.2	94.6	138	27.2	20.0	1.40	29.2	21.8	1.52	2.92	1.06	6
2.94	.432	1.876	.3	123	184	28.7	21.4	1.49	30.9	23.2	1.61	3.10	1.05	5
3.12	.423	1.895	.5	161	250	30.1	22.4	1.56	32.6	24.6	1.70	3.26	1.05	5
3.26	.419	1.897	.6	199	314	31.4	23.5	1.63	33.9	25.9	1.78	3.41	1.05	5
3.38	.416	1.902	1.1	248	395	32.6	24.6	1.70	35.2	27.2	1.85	3.55	1.05	5
3.48	.413	1.907	1.6	311	503	33.9	25.9	1.77	36.4	28.6	1.93	3.70	1.06	6
3.57	.411	1.907	2.4	367	599	34.8	26.8	1.83	37.3	29.7	1.99	3.82	1.07	7

[a]From corrected strains. Not used in computing M_{th}.
[b]Rotation clockwise in figure 16. Not used in computing M_{th}.
[c] $e_c = e_2$; $e_t = 1.138e_4$.
[d]Resisting moment of tension and compression areas computed separately by Cozzone's method assuming neutral axis stationary:

$$M_{th}' = \frac{I_{Nc}}{c_c}\frac{1}{\cos\phi}\left[f_{mc} + f_{0c}(k_c - 1)\right] = 0.0316(f_{mc} + 0.865f_{0c})$$

$$M_{th}'' = \frac{I_{Nt}}{c_t}\frac{1}{\cos\phi}\left[f_{mt} + f_{0t}(k_t - 1)\right] = 0.0319(f_{mt} + 0.840f_{0t})$$

$$M_{th} = M_{th}' + M_{th}''$$

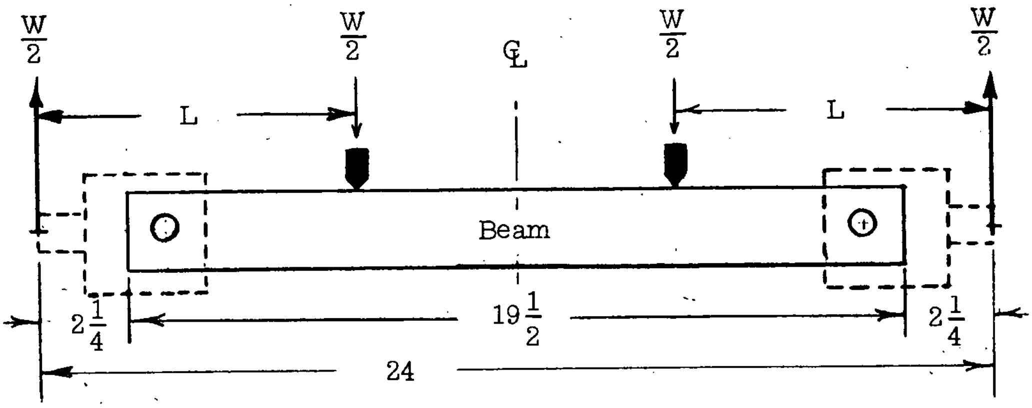

(a) Schematic loading arrangement.

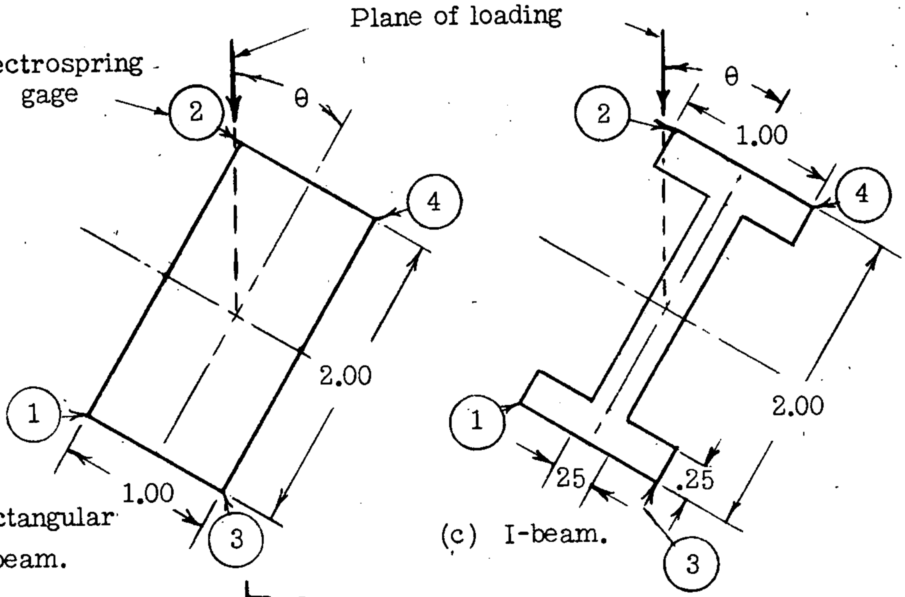

(b) Rectangular beam.

(c) I-beam.

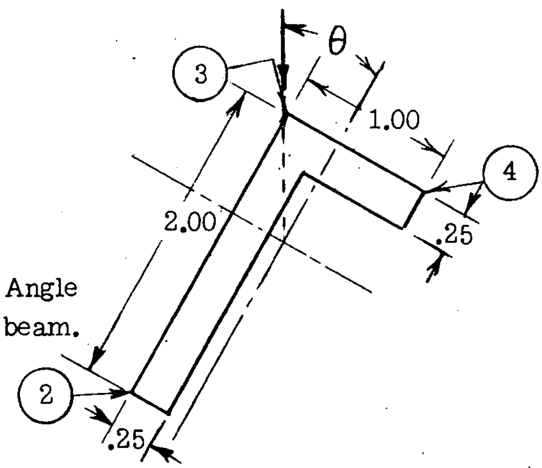

(d) Angle beam.

Figure 1.- Arrangement of loads, shapes of beam sections, and location of electrospring gages.

Page intentionally left blank

Page intentionally left blank

(a) Top view.

(b) Side view.

Figure 2.- Samples of tested specimens.

Page intentionally left blank

Page intentionally left blank

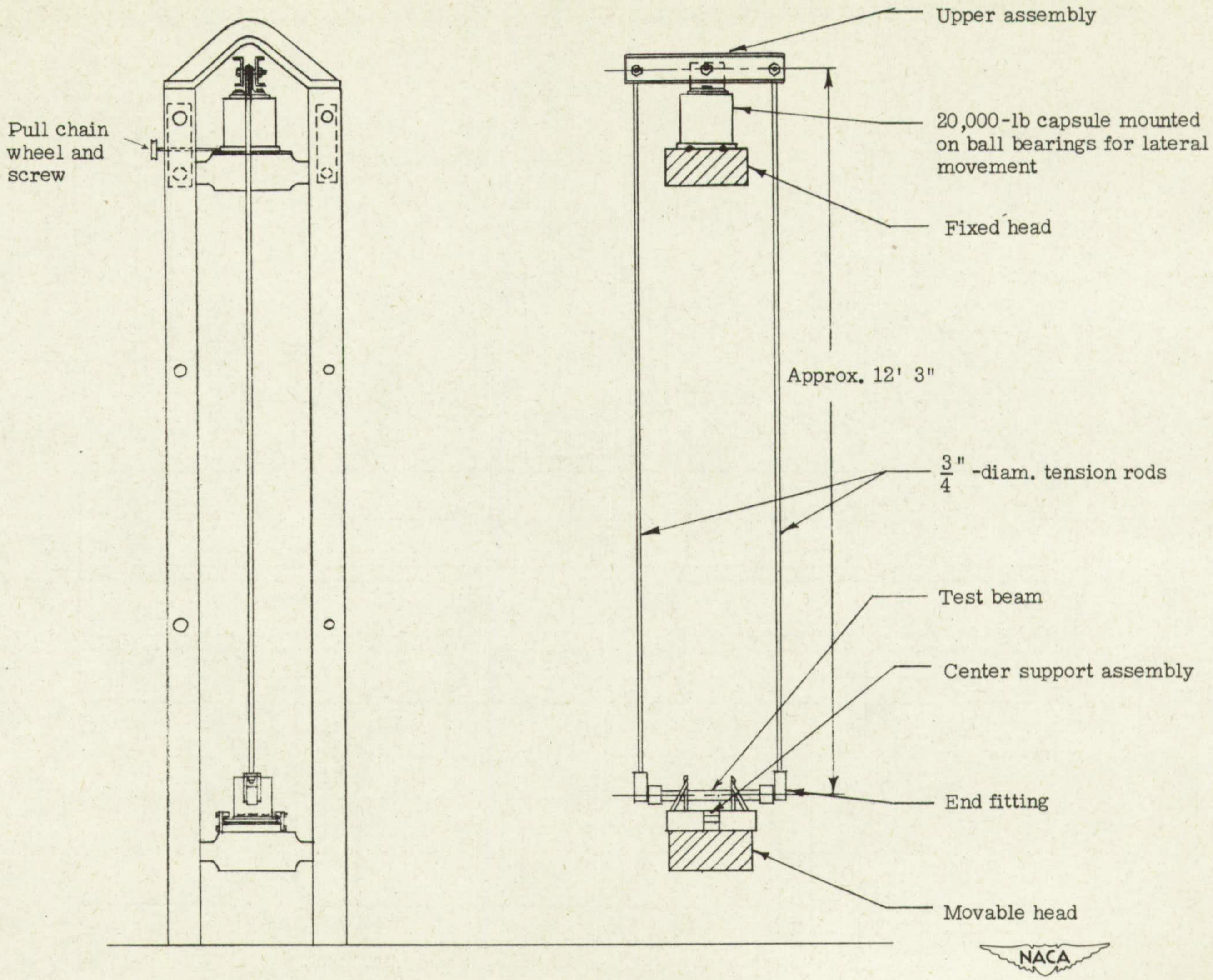

Figure 3.- Schematic arrangement of apparatus.

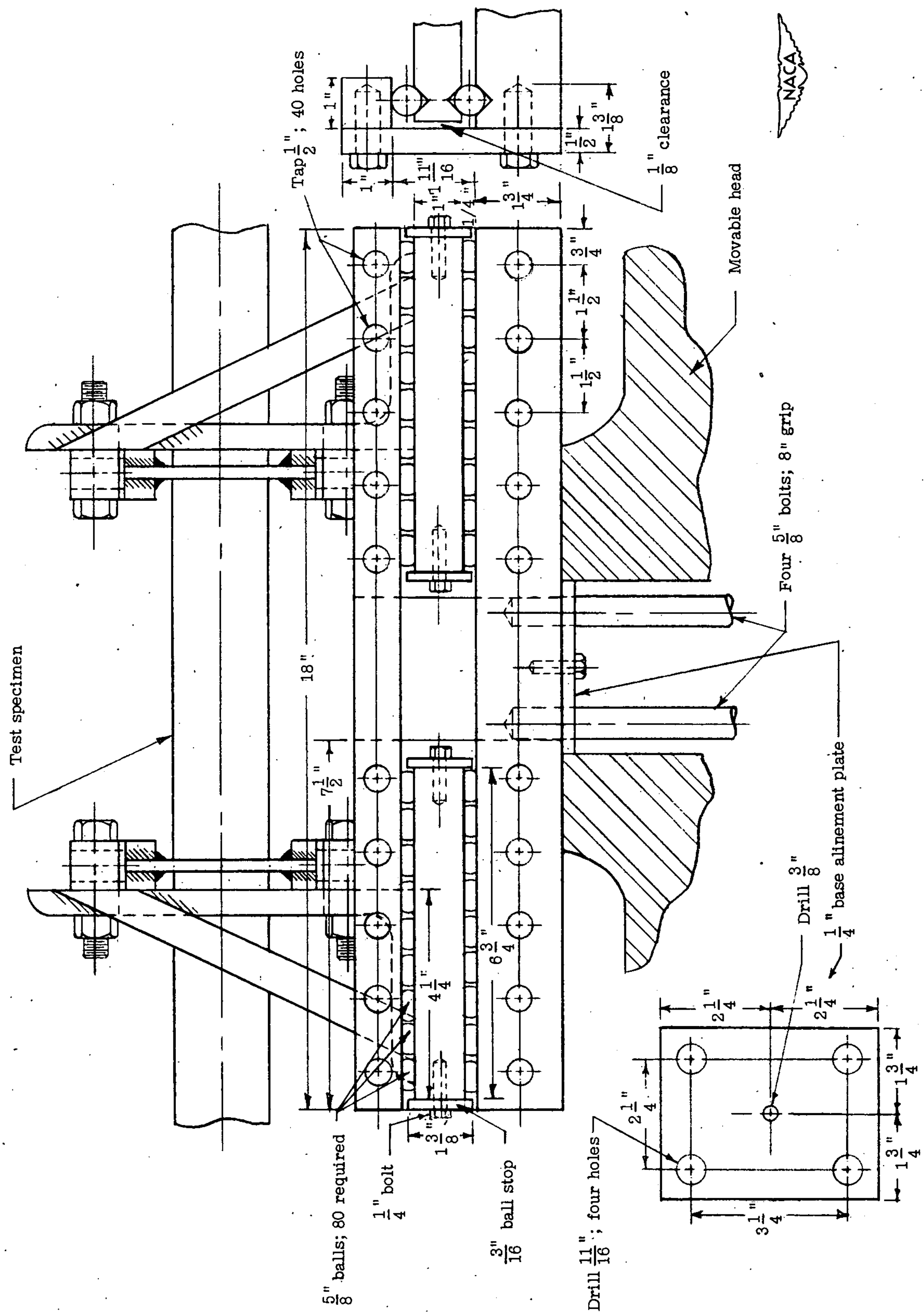

Figure 4.- Center support assembly. Near retaining plate has been removed for clarity.

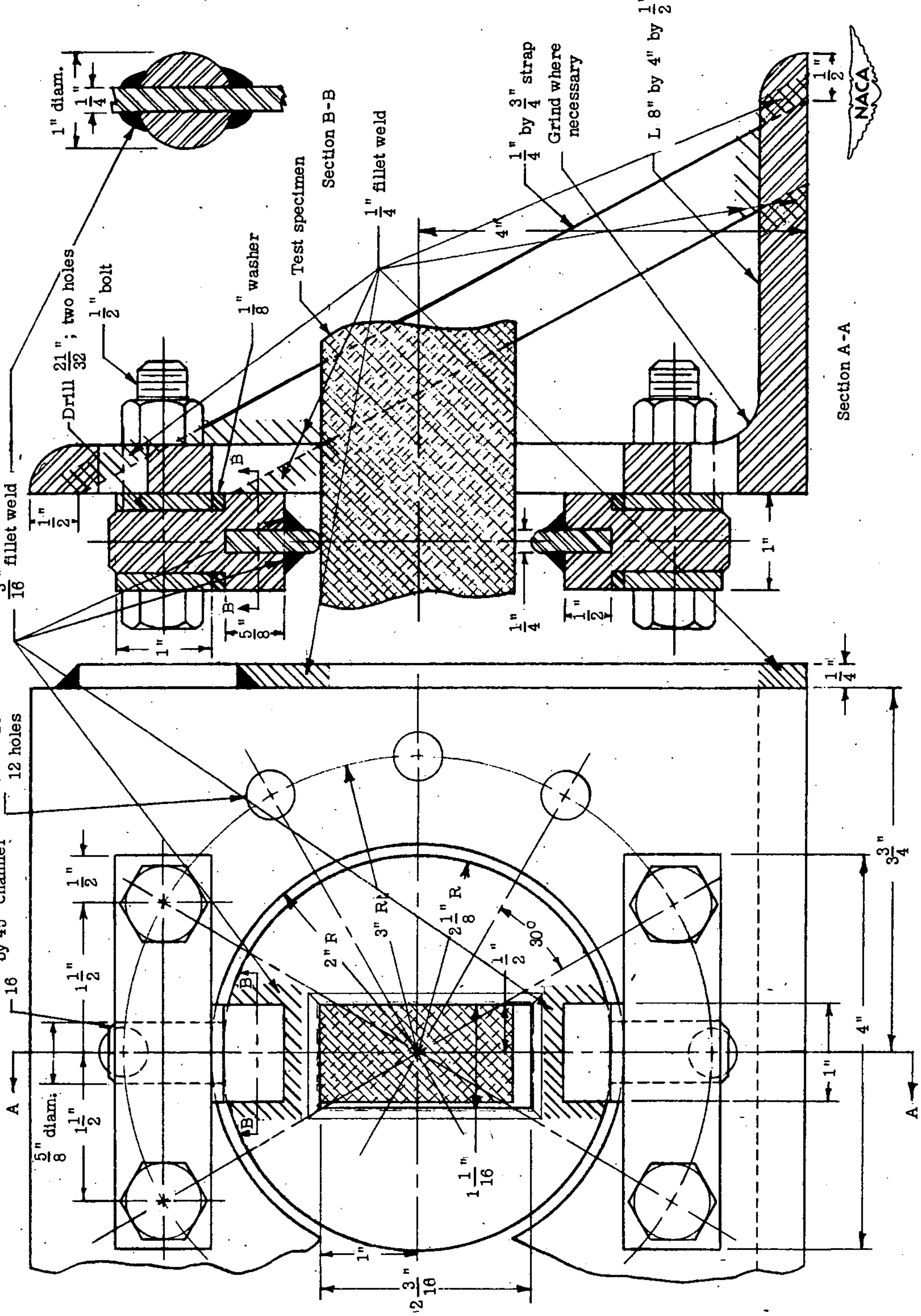

Figure 5.- Details of third-point loading device.

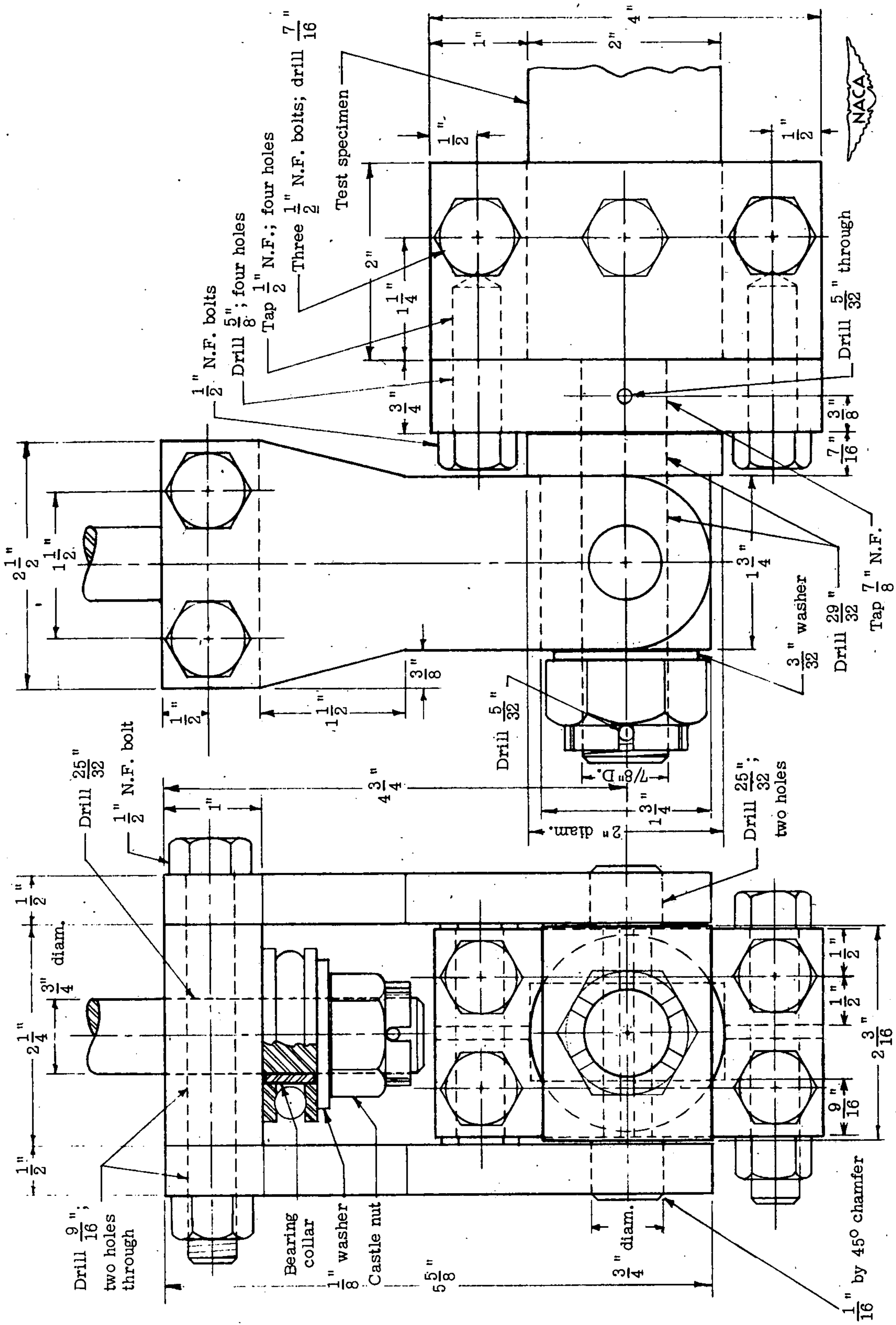

Figure 6.- Details of end fitting.

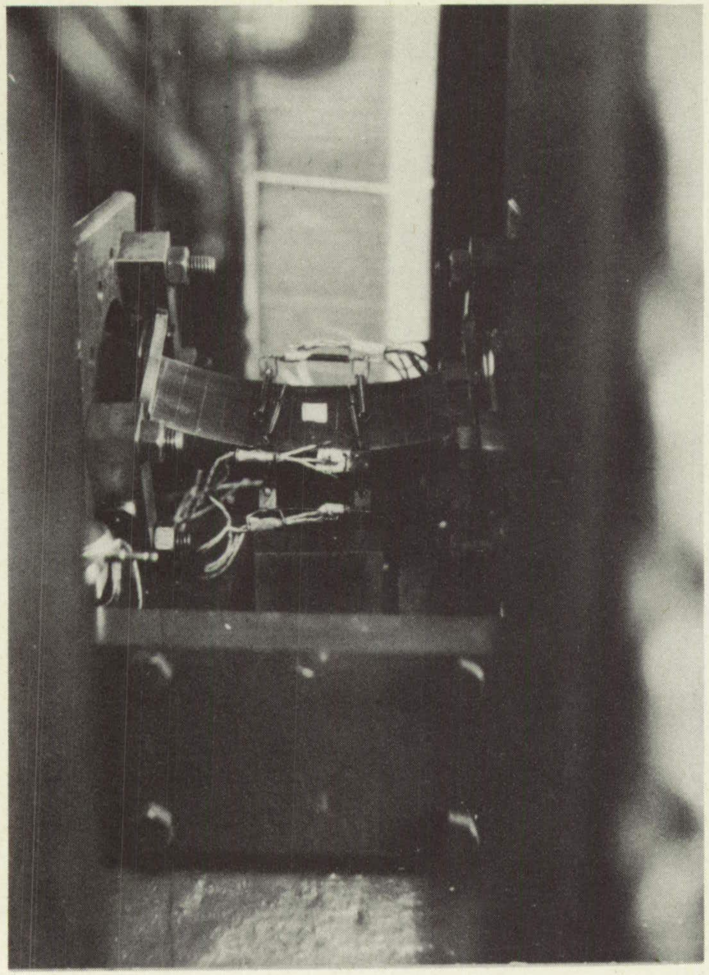

Figure 7.- Rectangular beam under test in loading jig.

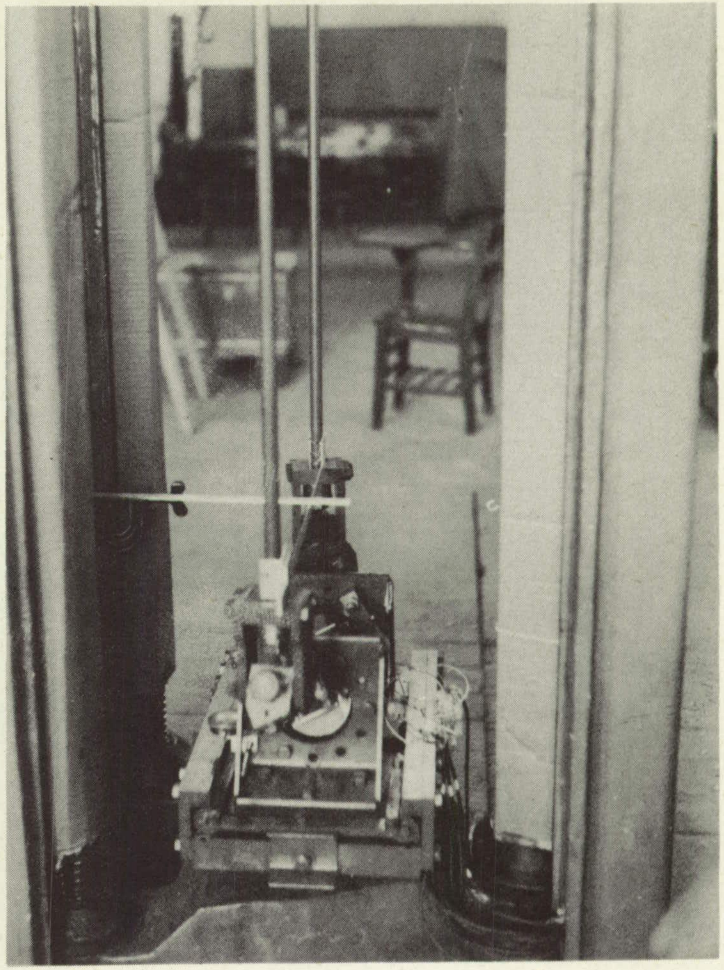

Figure 8.- Loading jig and end support fittings.

Page intentionally left blank

Page intentionally left blank

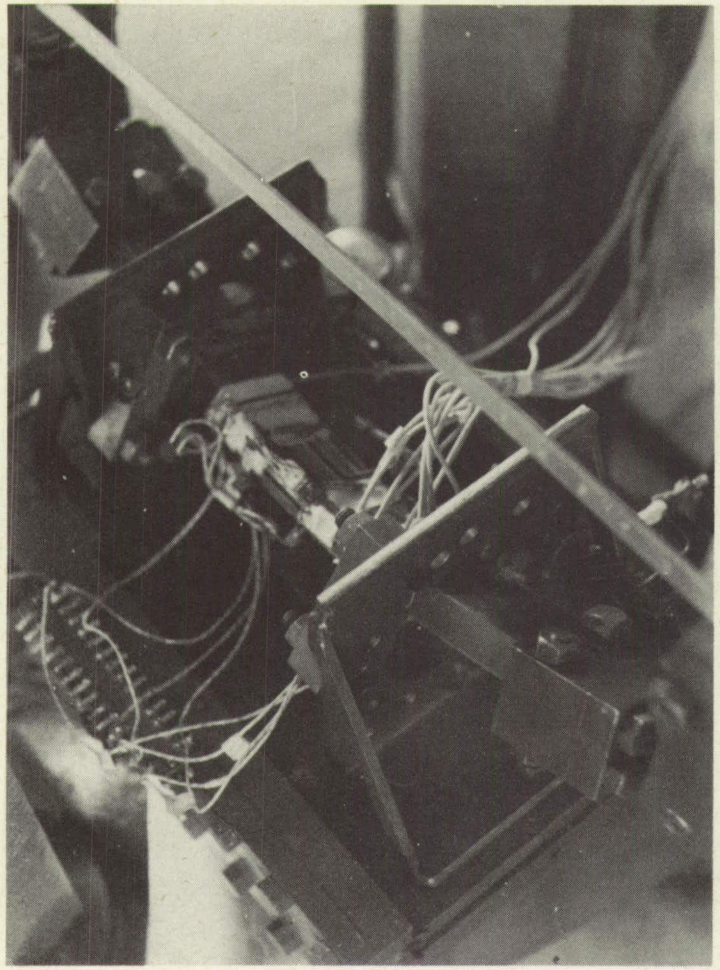

Figure 9.- Electrospring gages mounted on rectangular beam under test.

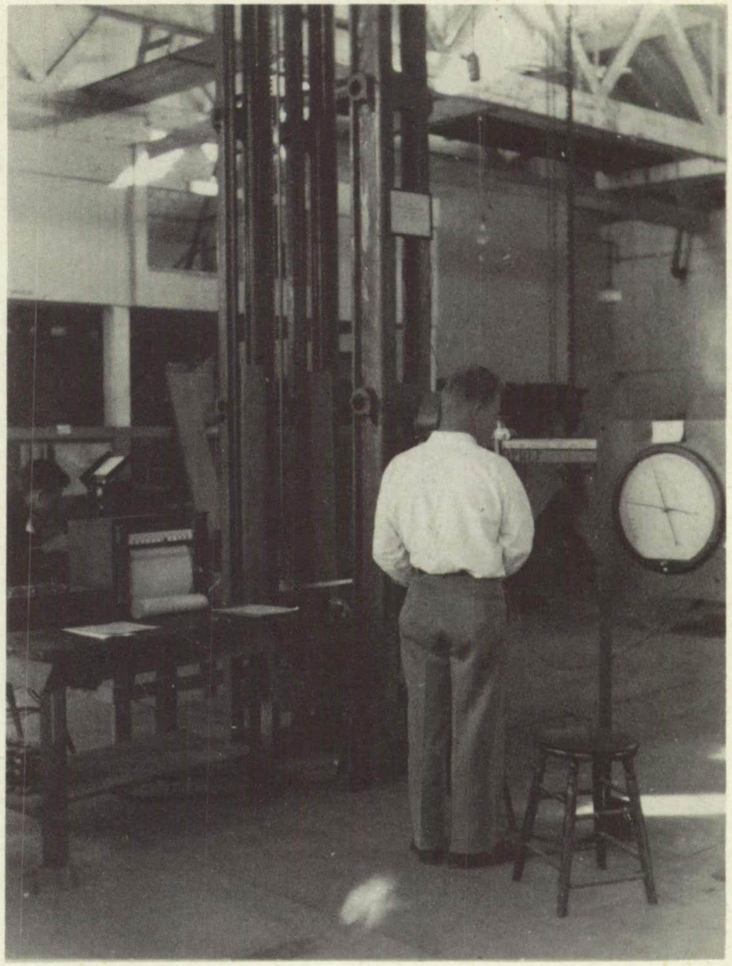

Figure 10.- Arrangement of testing apparatus.

Page intentionally left blank

Page intentionally left blank

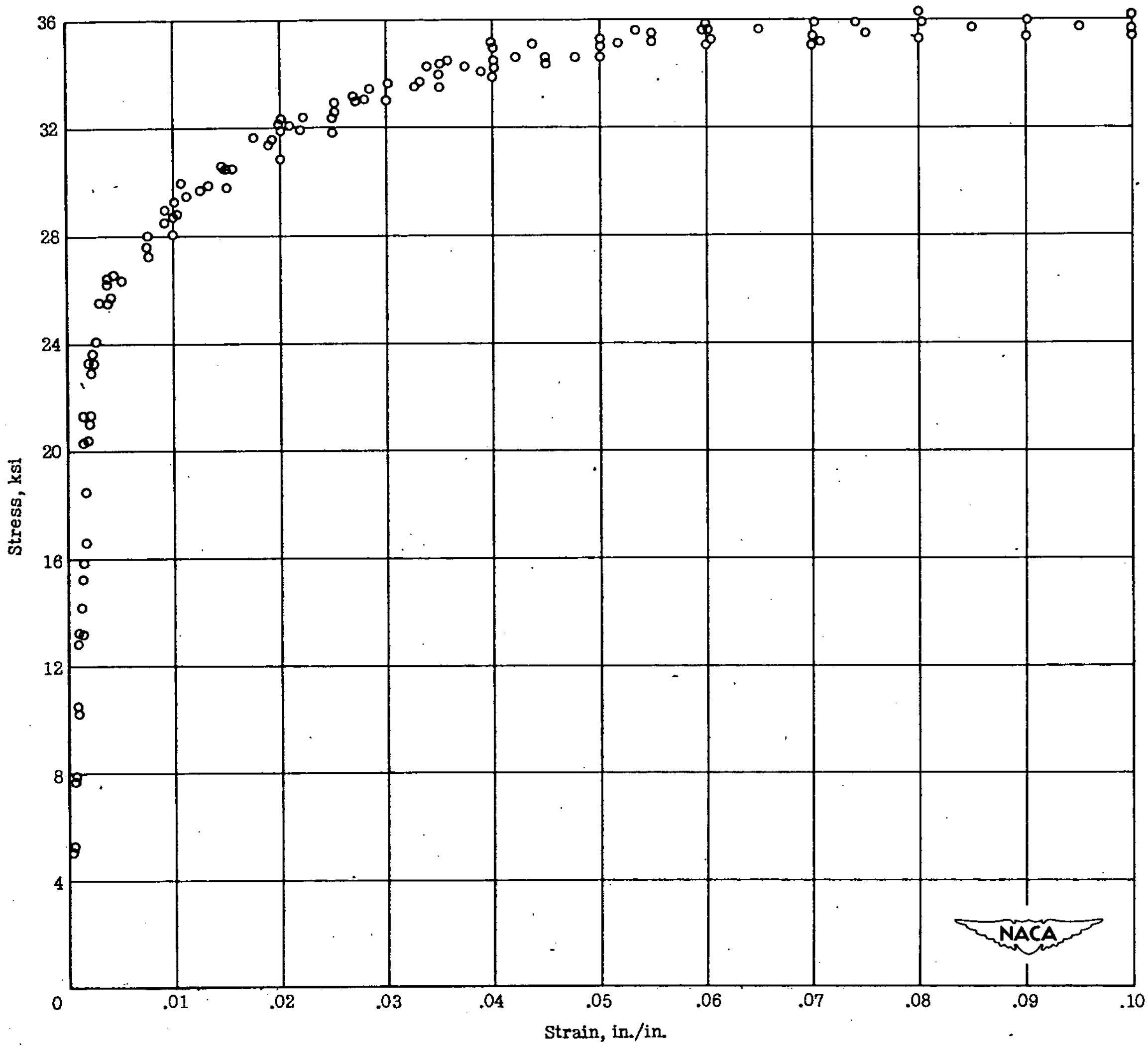

Figure 11.- Tension test results. Material, aluminum alloy 75S-0; results from coupons 0.125 inch thick and 0.500 inch wide at reduced section.

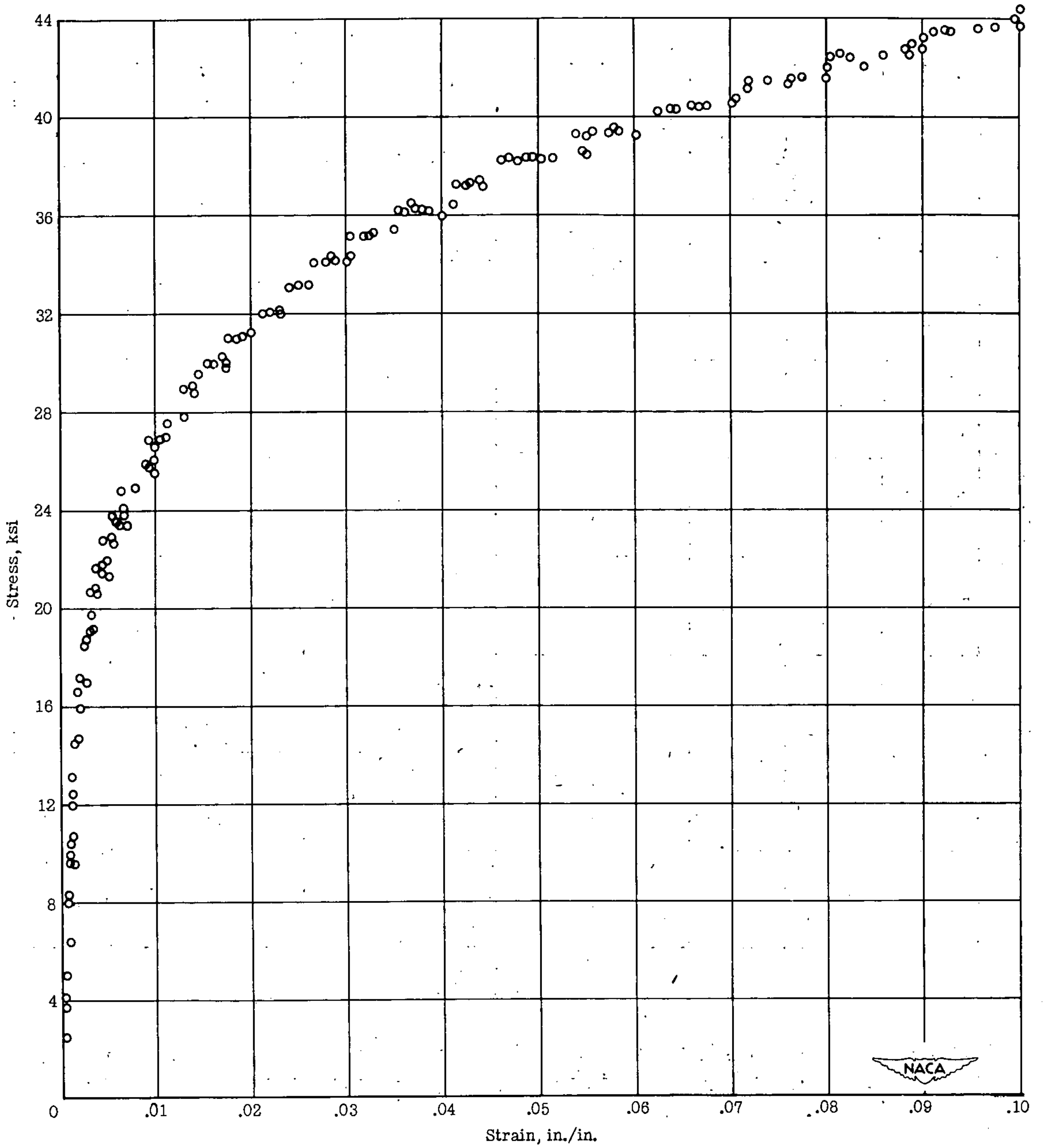

Figure 12.- Compression test results. Material, aluminum alloy 75S-0; results from block coupons 1 by 15/16 by 3 inches.

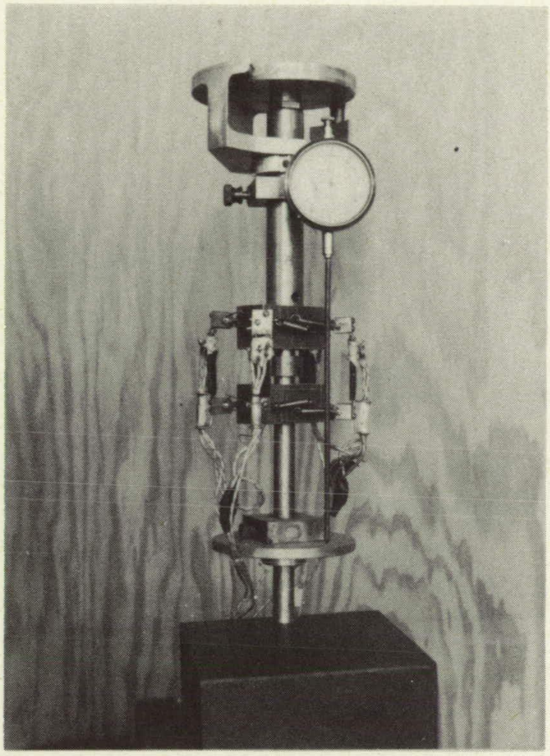

Figure 13.- Electrospring gages mounted on calibration apparatus.

Page intentionally left blank

Page intentionally left blank

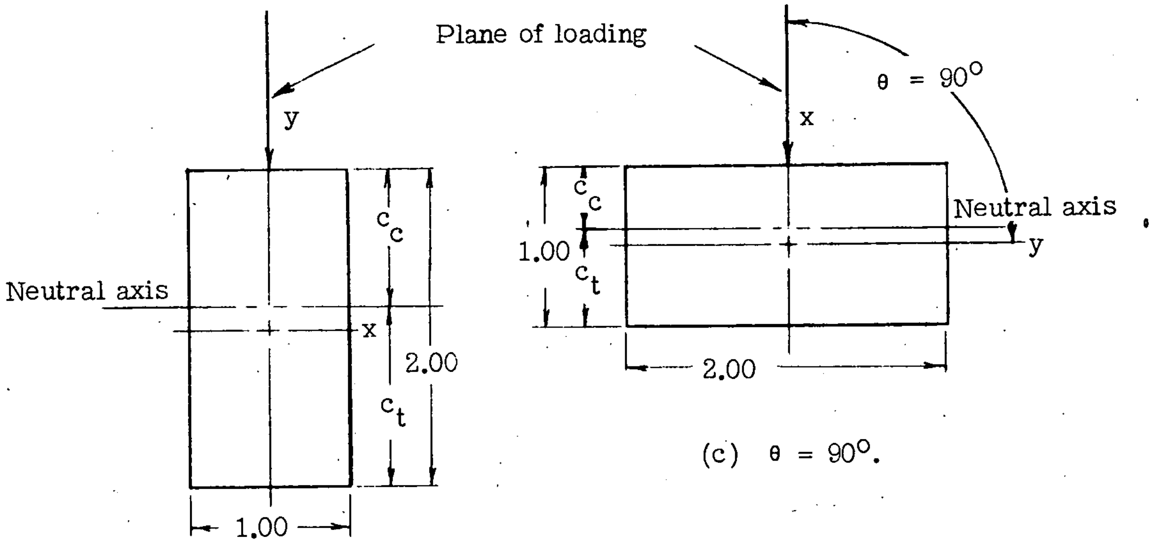

(a) $\theta = 0^{\circ}$.

(c) $\theta = 90^{\circ}$.

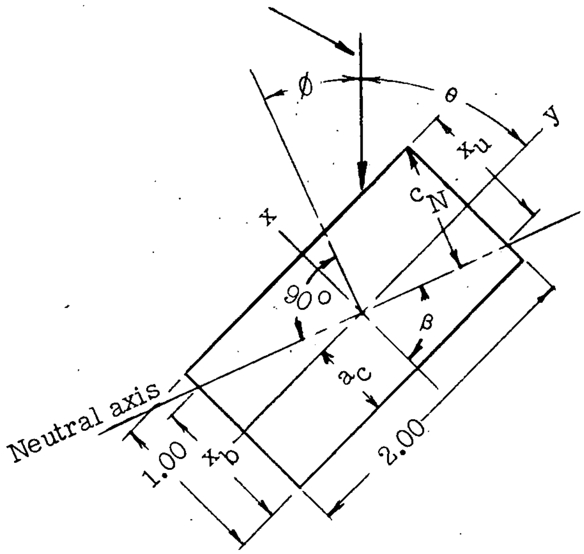

Section properties					
I_x = 0.667 in.^{4}					
I_y = 0.167 in.^{4}					
θ	β	ϕ	I_N	Q_m	c_N
30°	66° 35'	36° 35'	0.242	0.287	0.852
60°	81° 47'	21° 47'	.177	.252	.640

NACA

(b) θ = 30° or 60°.

Figure 14.- Rectangular beam sections.

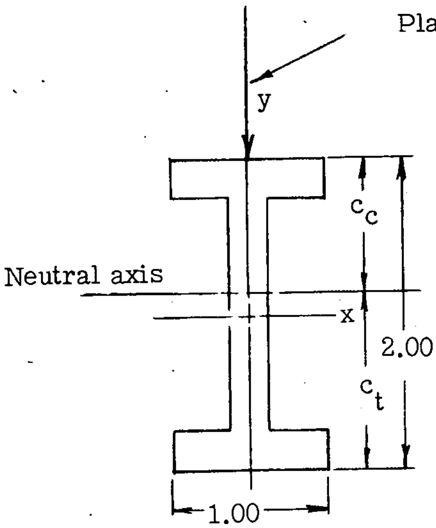

(a) $\theta = 0^{\circ}$.

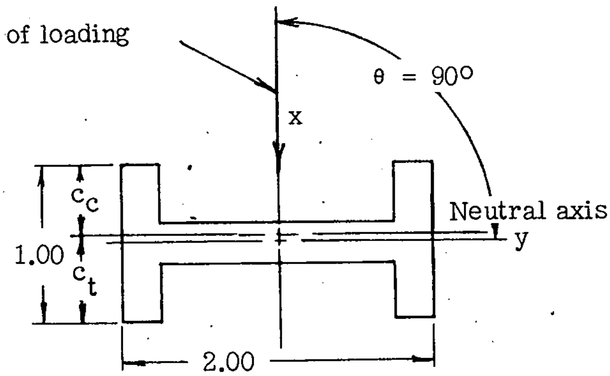

(c) $\theta = 90^{\circ}$.

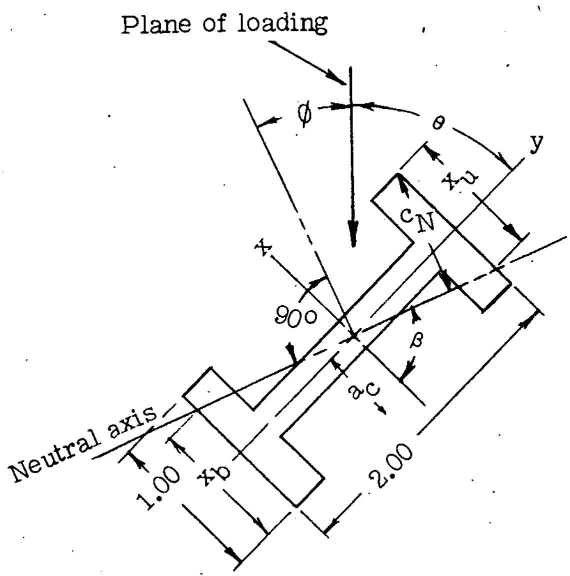

(b) $\theta = 30^{\circ}$ or 60°.

Section properties					
$I_x = 0.456$					
$I_y = 0.0436$					
θ	β	ϕ	I_N	Q_m	c_N
30°	80° 35'	50° 35'	0.0546	0.0847	0.657
60°	86° 51'	26° 51'	.0443	.0767	.554

NACA

Figure 15.- I-beam sections.

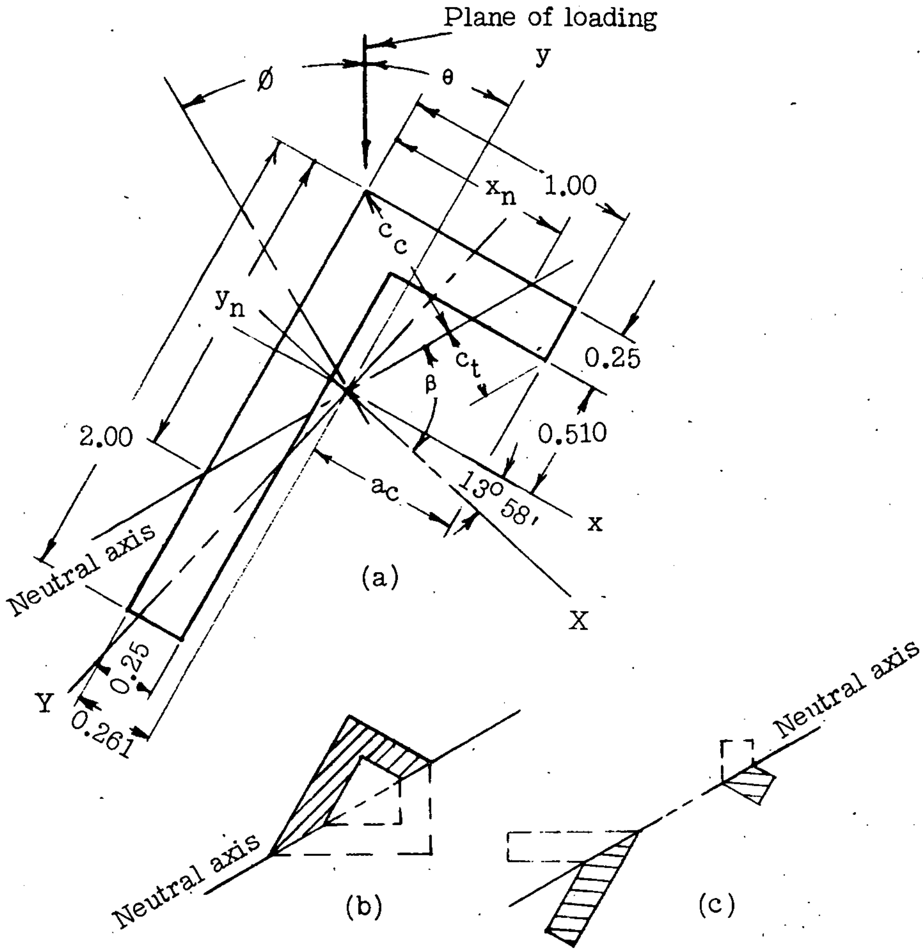

Section properties								
Rectangular axes				Principal axes				
I_x = 0.2706 I_y = 0.0456 I_{xy} = 0.0600				I_X = 0.2854 I_Y = 0.0308				
θ	β	Ø	I_c	I_t	Q_{mc}	Q_{mt}	c_c	c_t
0°	66° 33'	52° 35'	0.0330	0.0385	0.0929	0.0862	0.670	[a]0.744
30°	83° 37'	39° 39'	.0167	.0173	.0635	.0622	.507	.518
60°	88° 13'	14° 15'	.0140	.0177	.0581	.0558	.457	.572
90°	91° 32'	12° 26'	.0117	.0194	.0555	.0584	.416	.646

[a]Distance to lower corner of 2-in. leg.

Figure 16.- Angle beam sections.

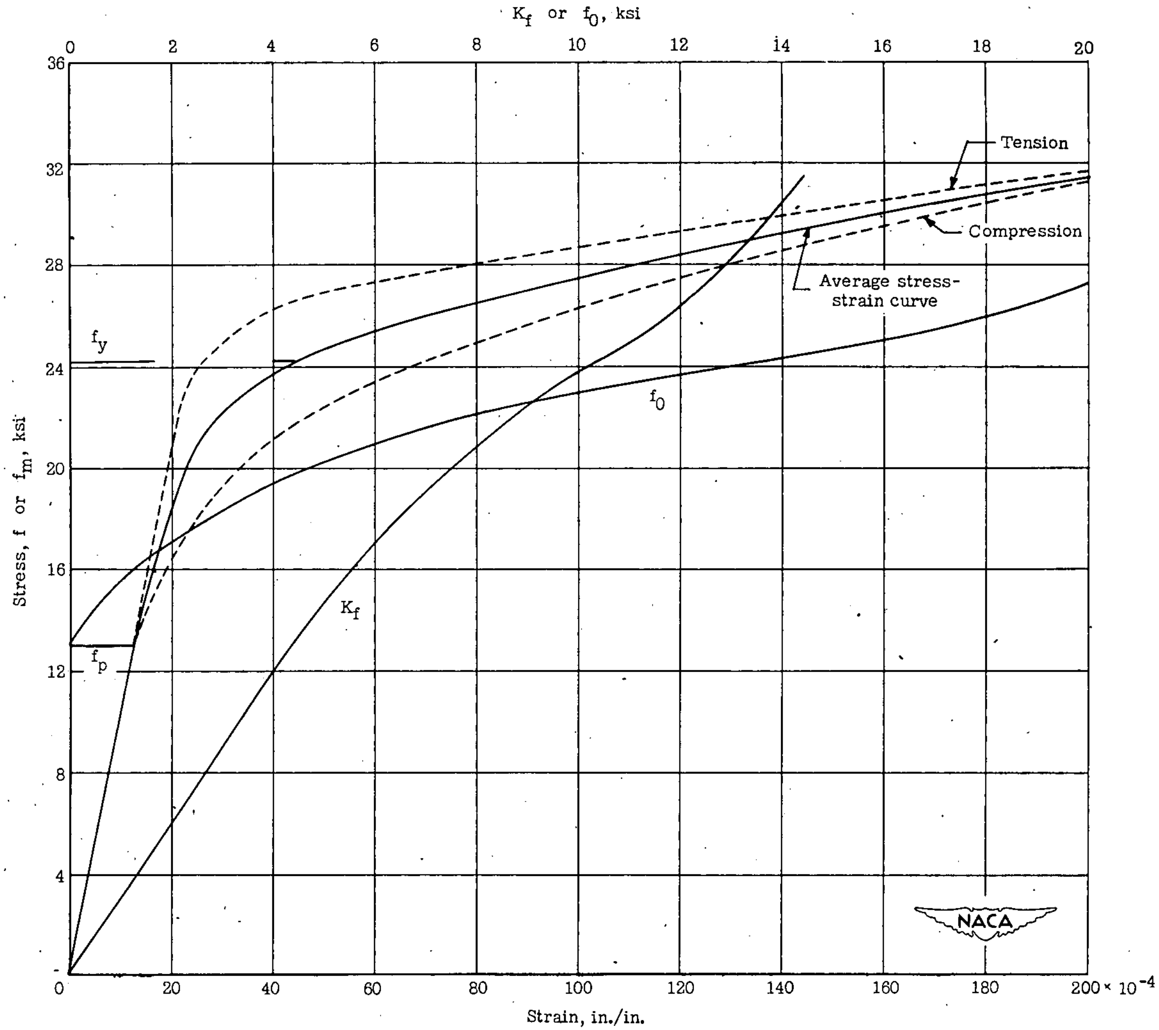

Figure 17.- Relationship between stress, strain, intercept stress, and plastic bending factor based on average stress-strain curve. Strains plotted to enlarged scale to facilitate reading; material, aluminum alloy 75S-0.

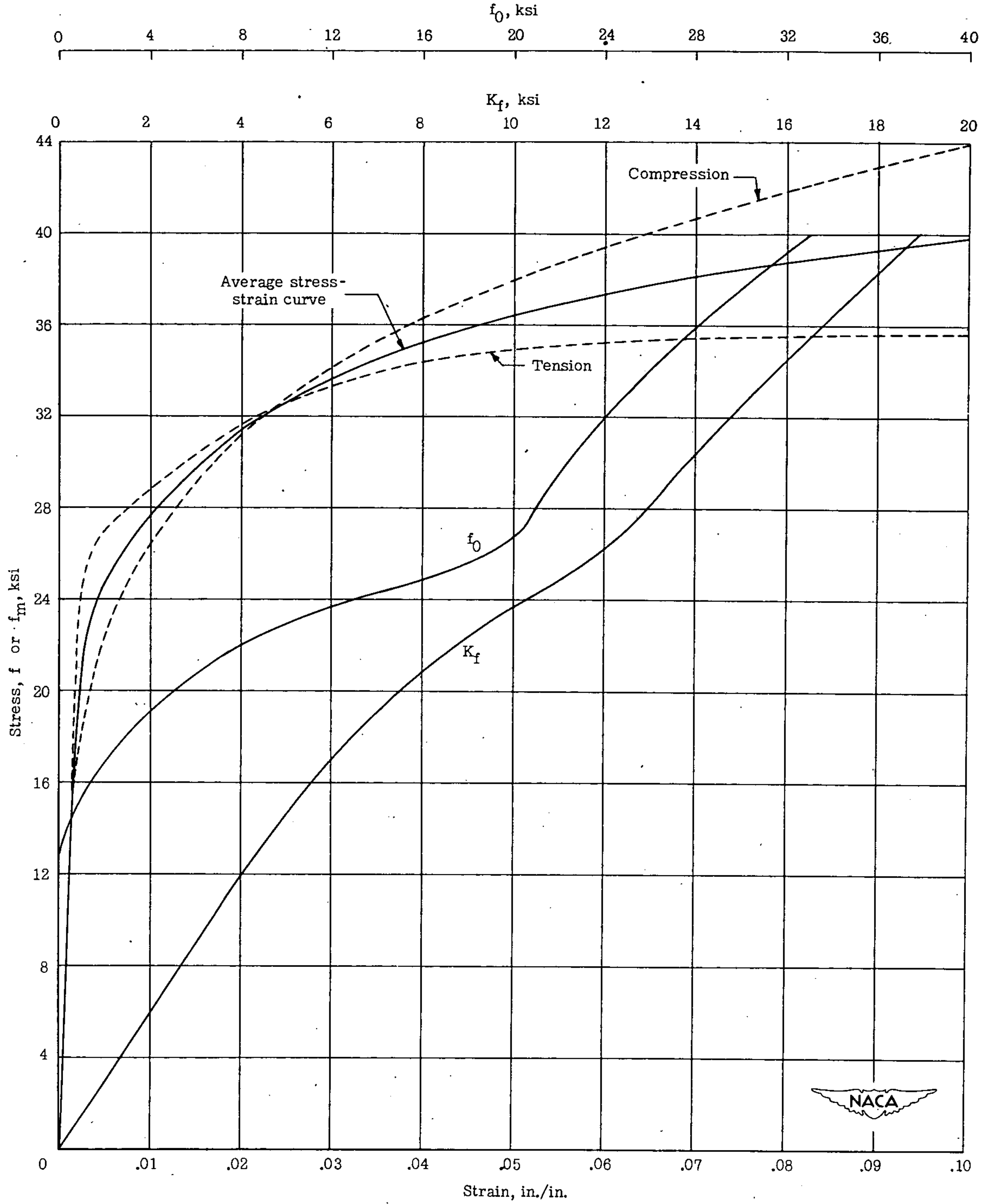

Figure 18.- Relationship between stress, strain, intercept stress, and plastic bending factor based on average stress-strain curve. Material, aluminum alloy 75S-0.

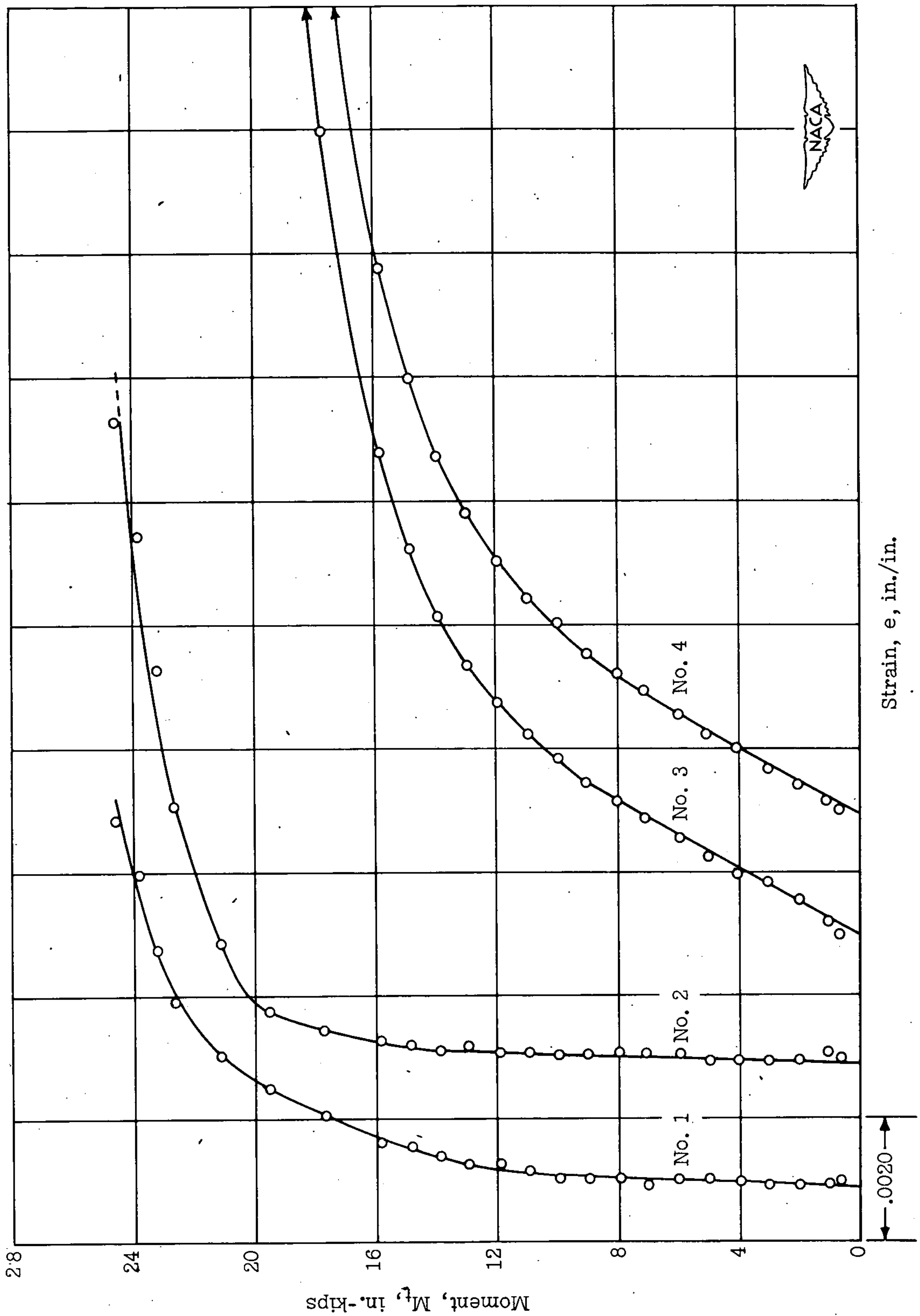

Figure 19.- Typical moment-strain curves for rectangular beam A-6. $\theta = 30^{\circ}$.

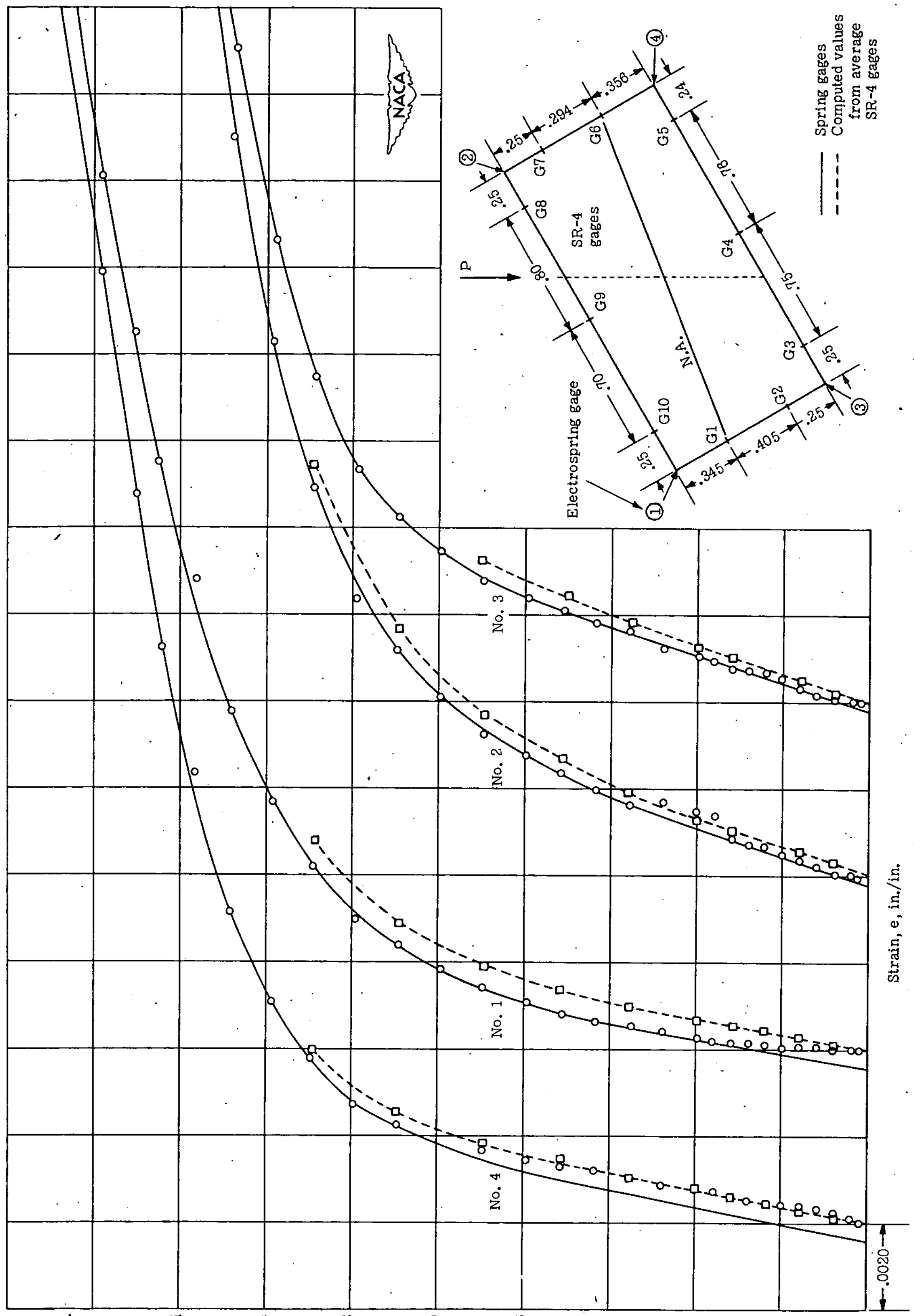

Figure 20.- Typical moment-strain curves for rectangular beam G-1. $\theta = 60^{\circ}$.

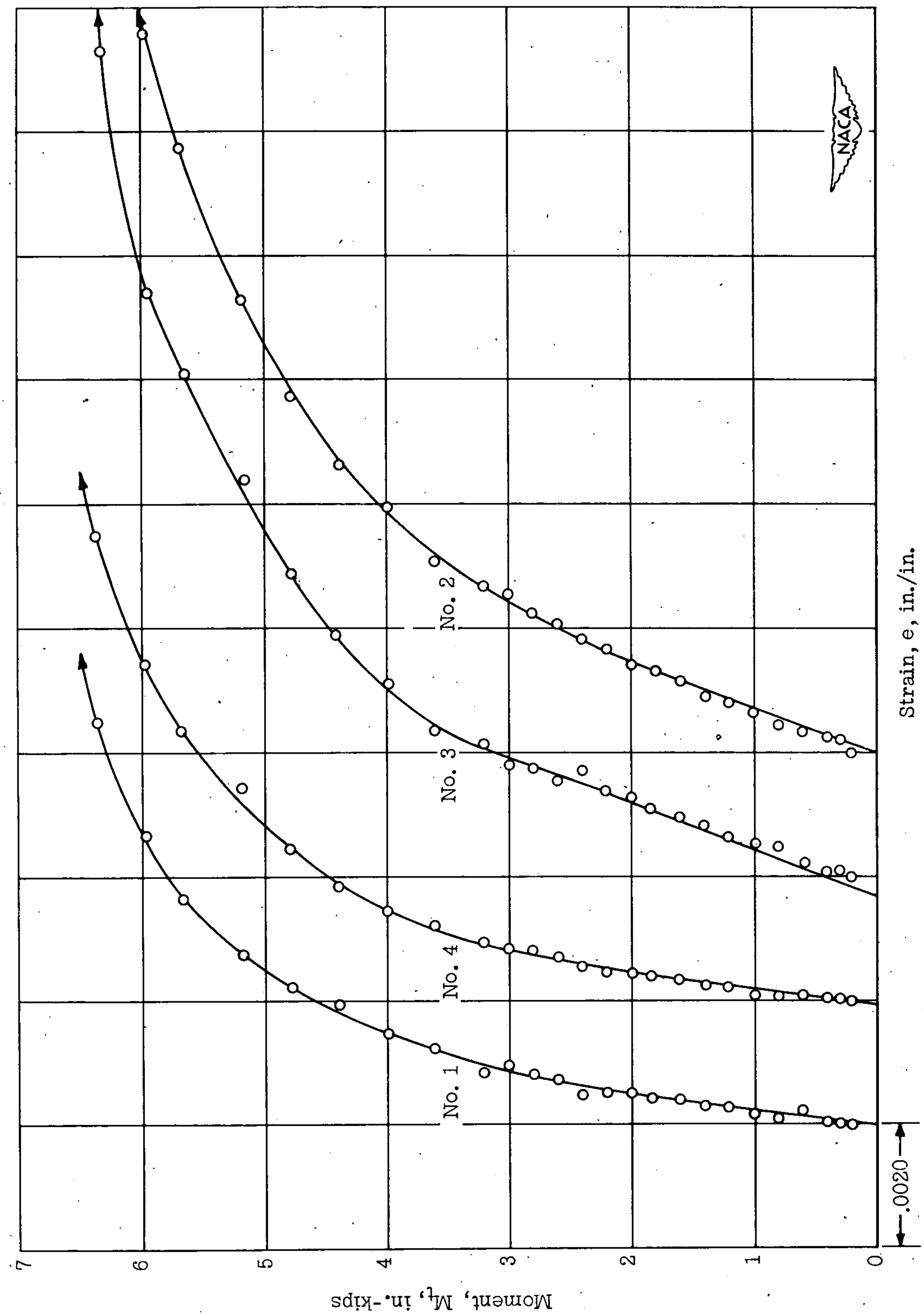

Figure 21.- Typical moment-strain curves for I-beam C-5. $\theta = 30°$.

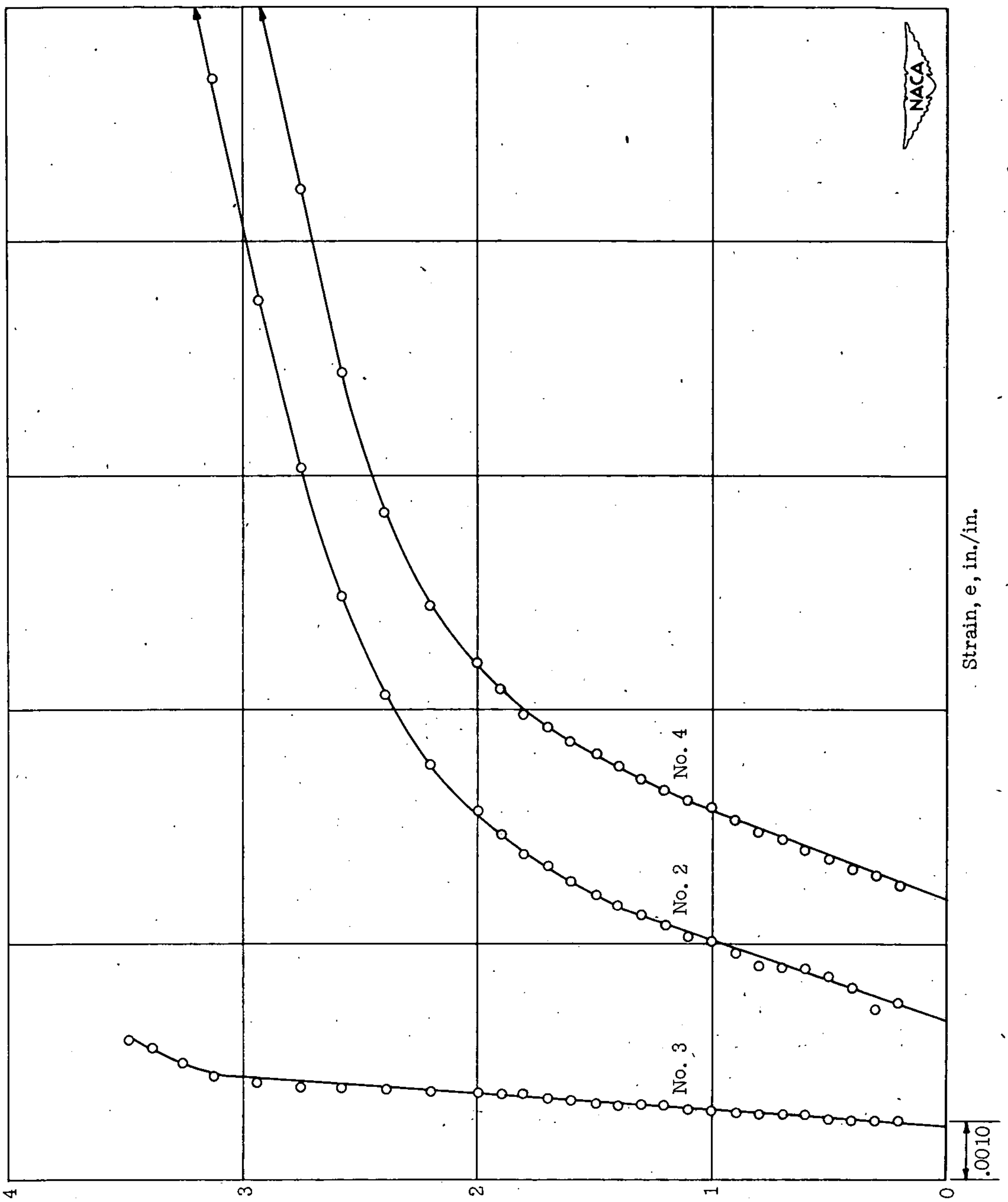

Figure 22.- Typical moment-strain curves for angle beam F-2. $\theta = 60^{\circ}$.

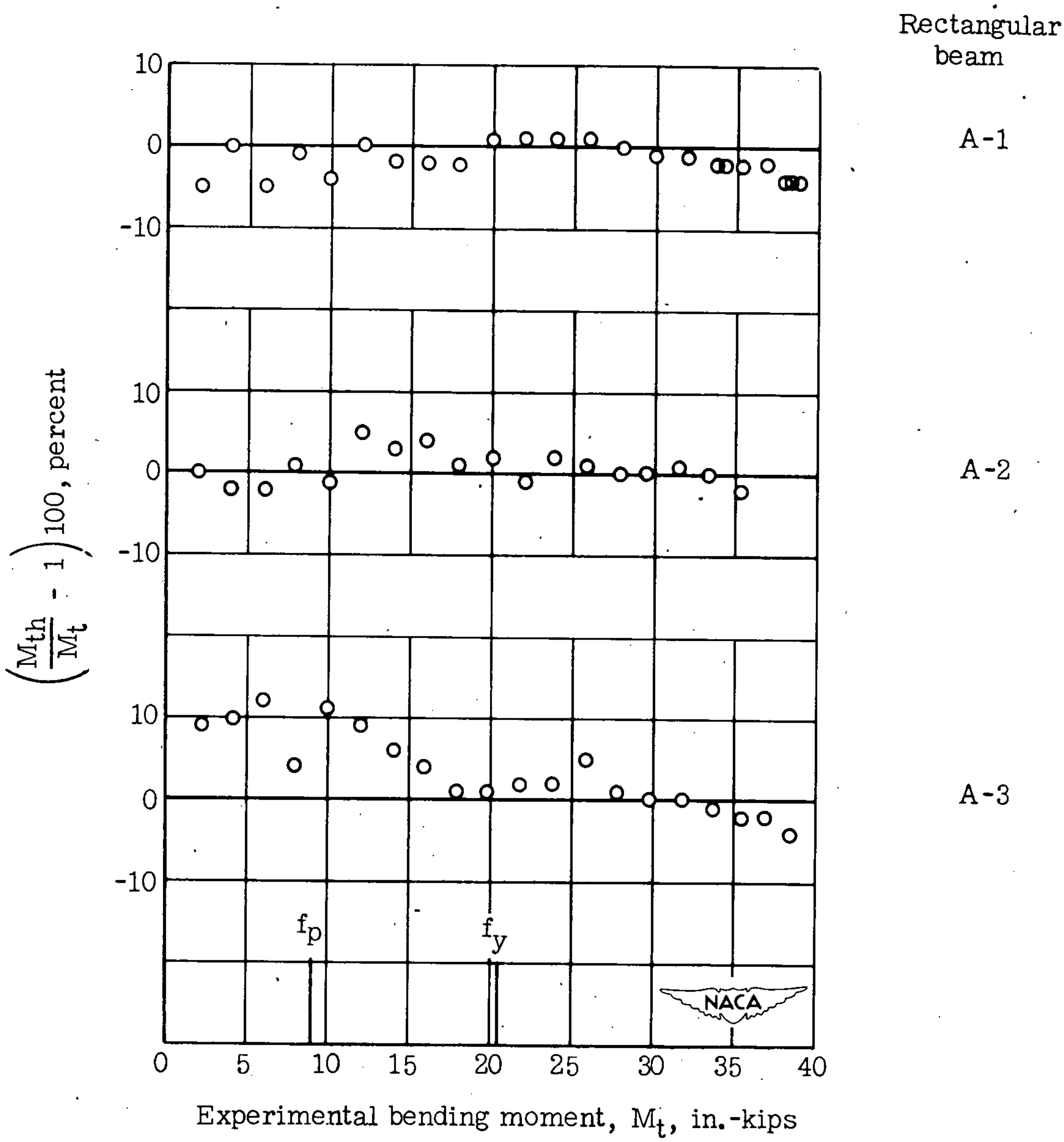

(a) $\theta = 0^{\circ}$.

Figure 23.- Difference between experimental and computed bending moments for rectangular beams.

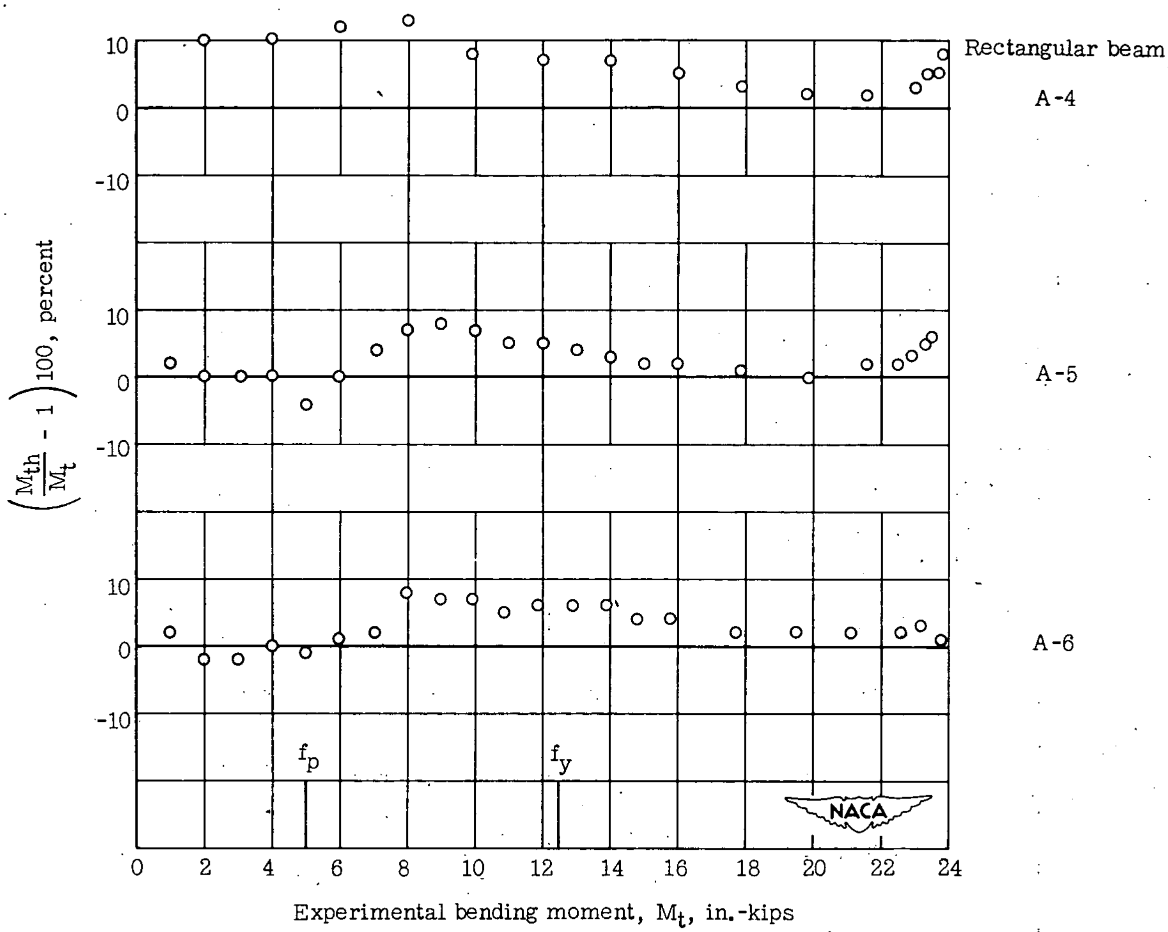

(b) $\theta = 30^{\circ}$.

Figure 23.- Continued.

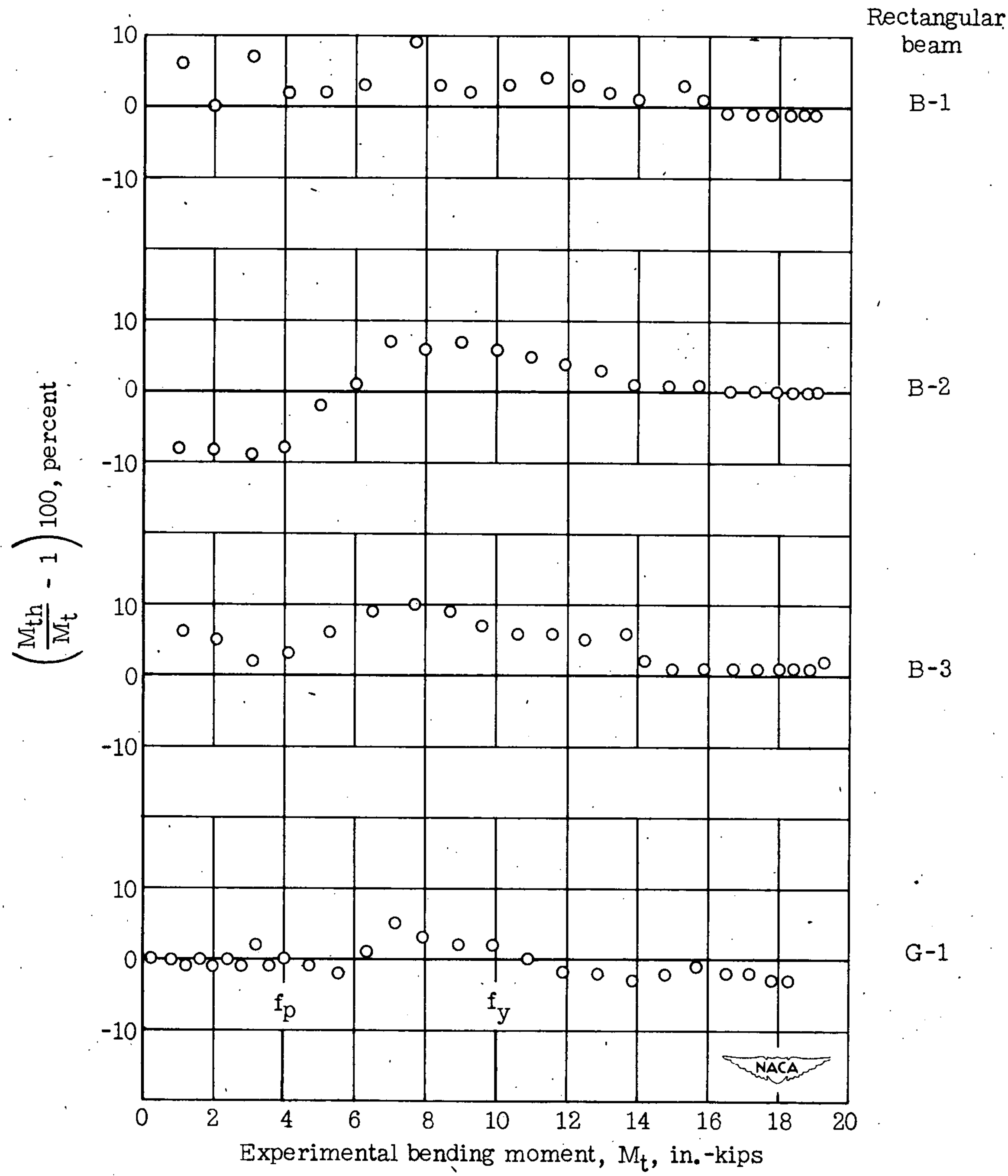

(c) $\theta = 60^{\circ}$.

Figure 23.- Continued.

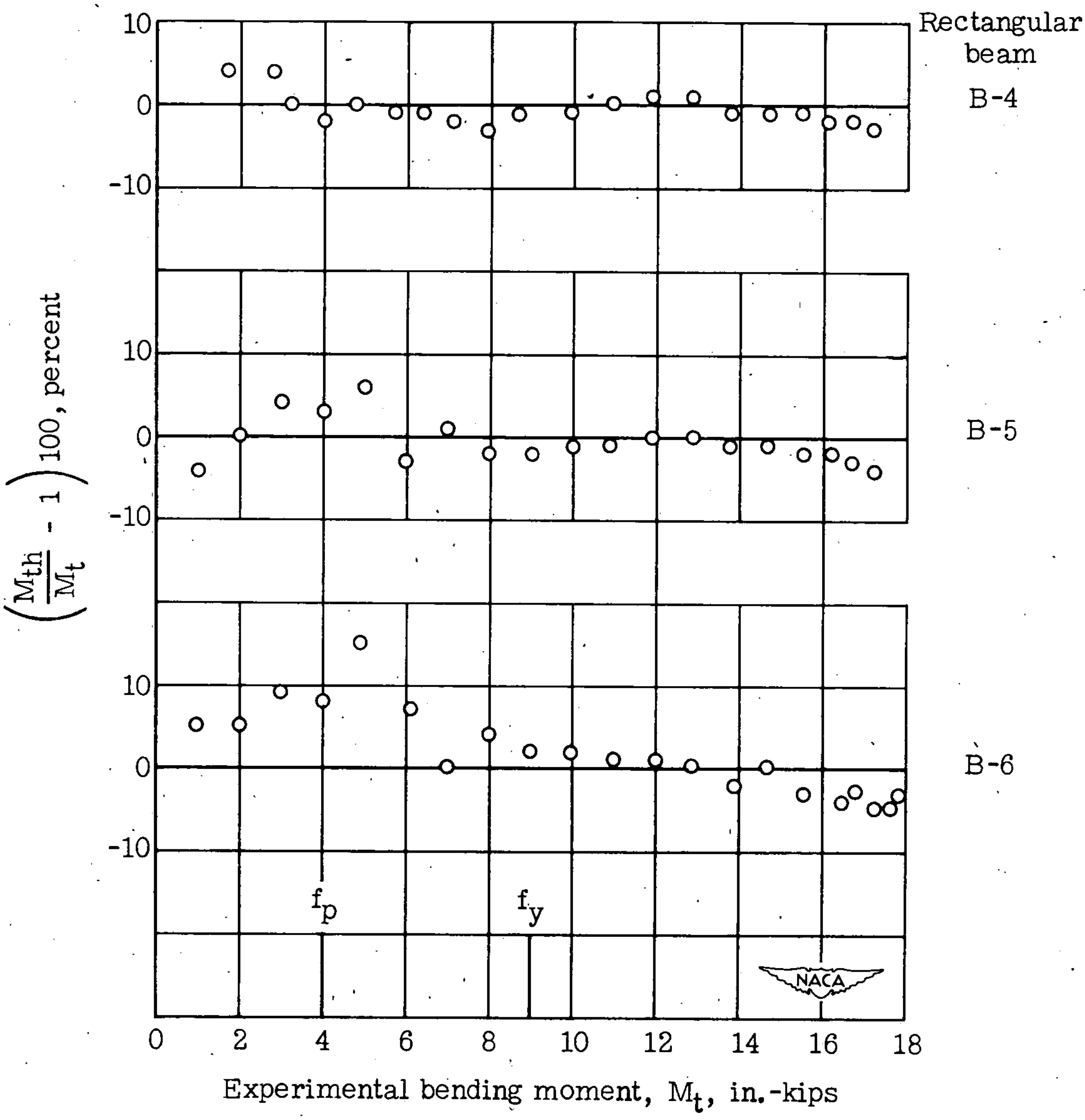

(d) $\theta = 90^{\circ}$.

Figure 23.- Concluded.

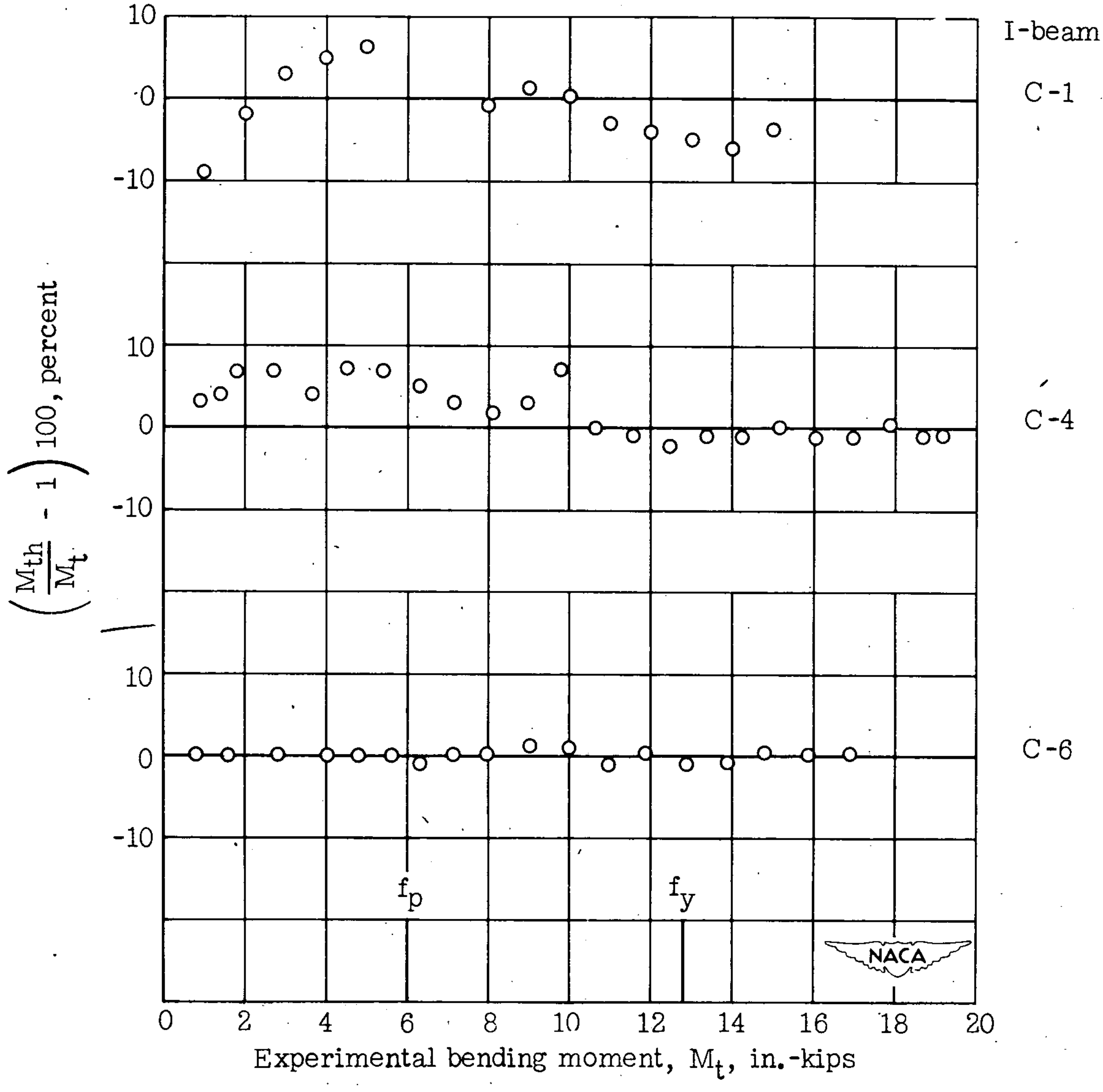

(a) $\theta = 0^{\circ}$.

Figure 24.- Difference between experimental and computed bending moments for I-beams.

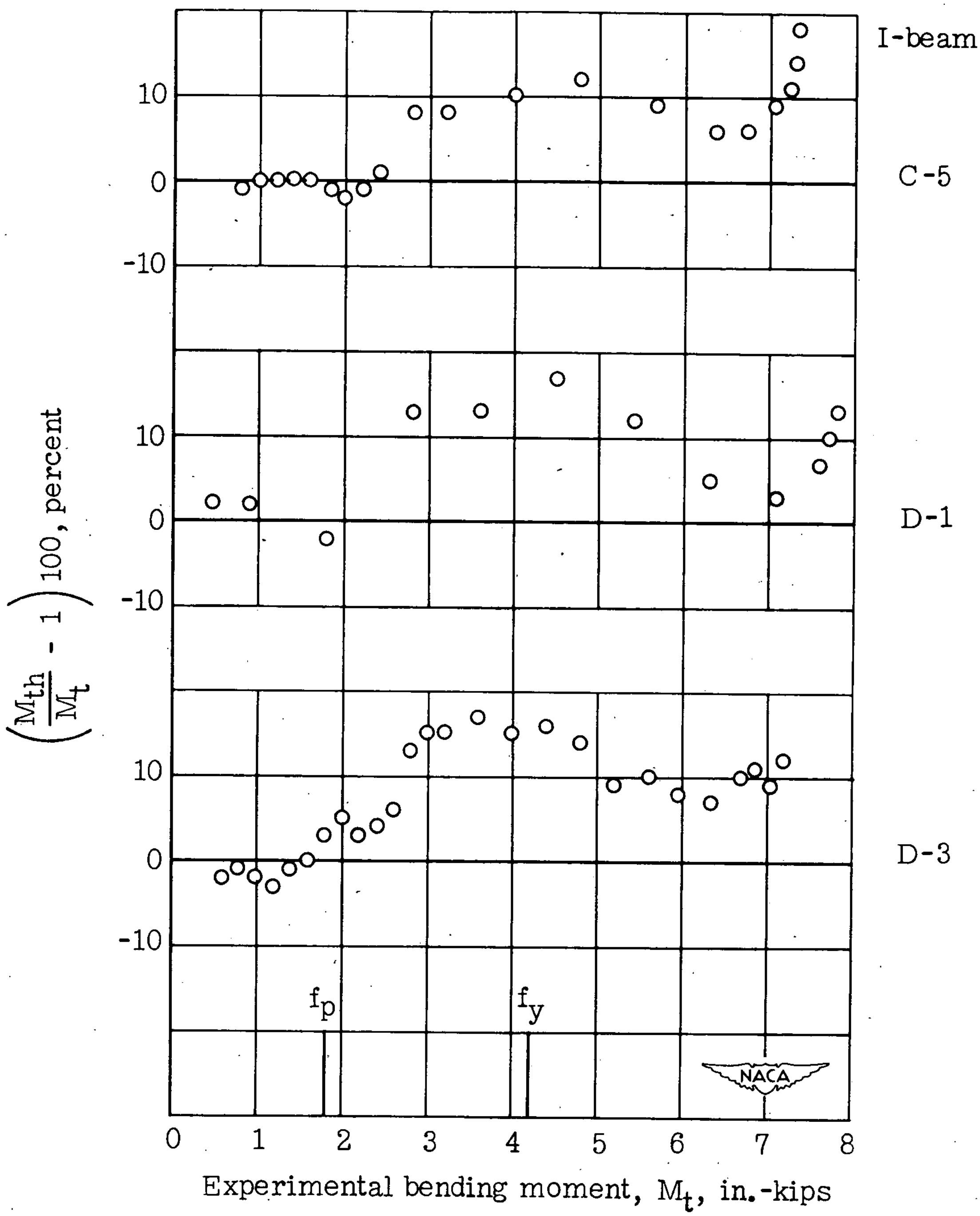

(b) $\theta = 30^{\circ}$.

Figure 24.- Continued.

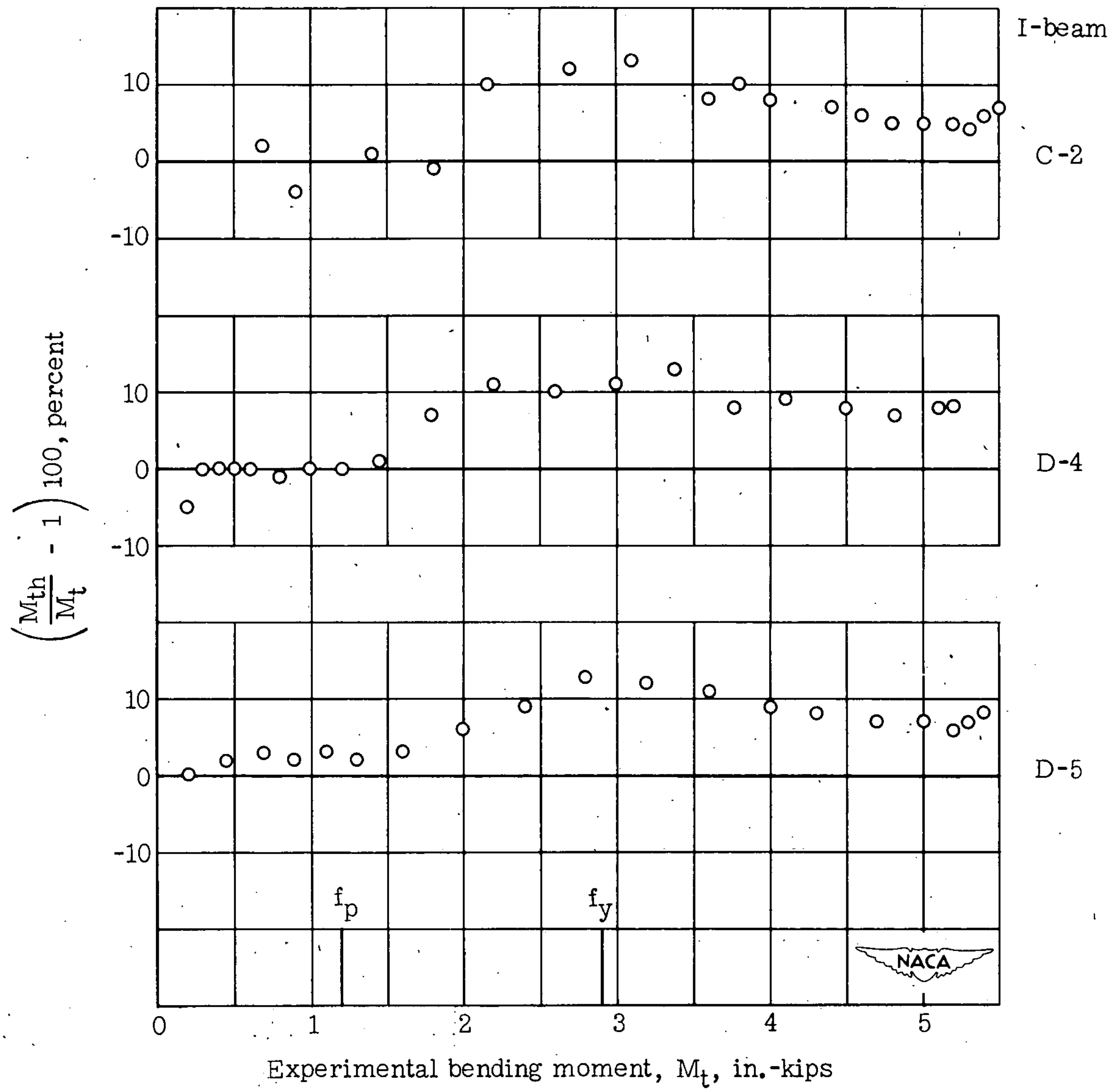

(c) $\theta = 60^{\circ}$.

Figure 24.- Continued.

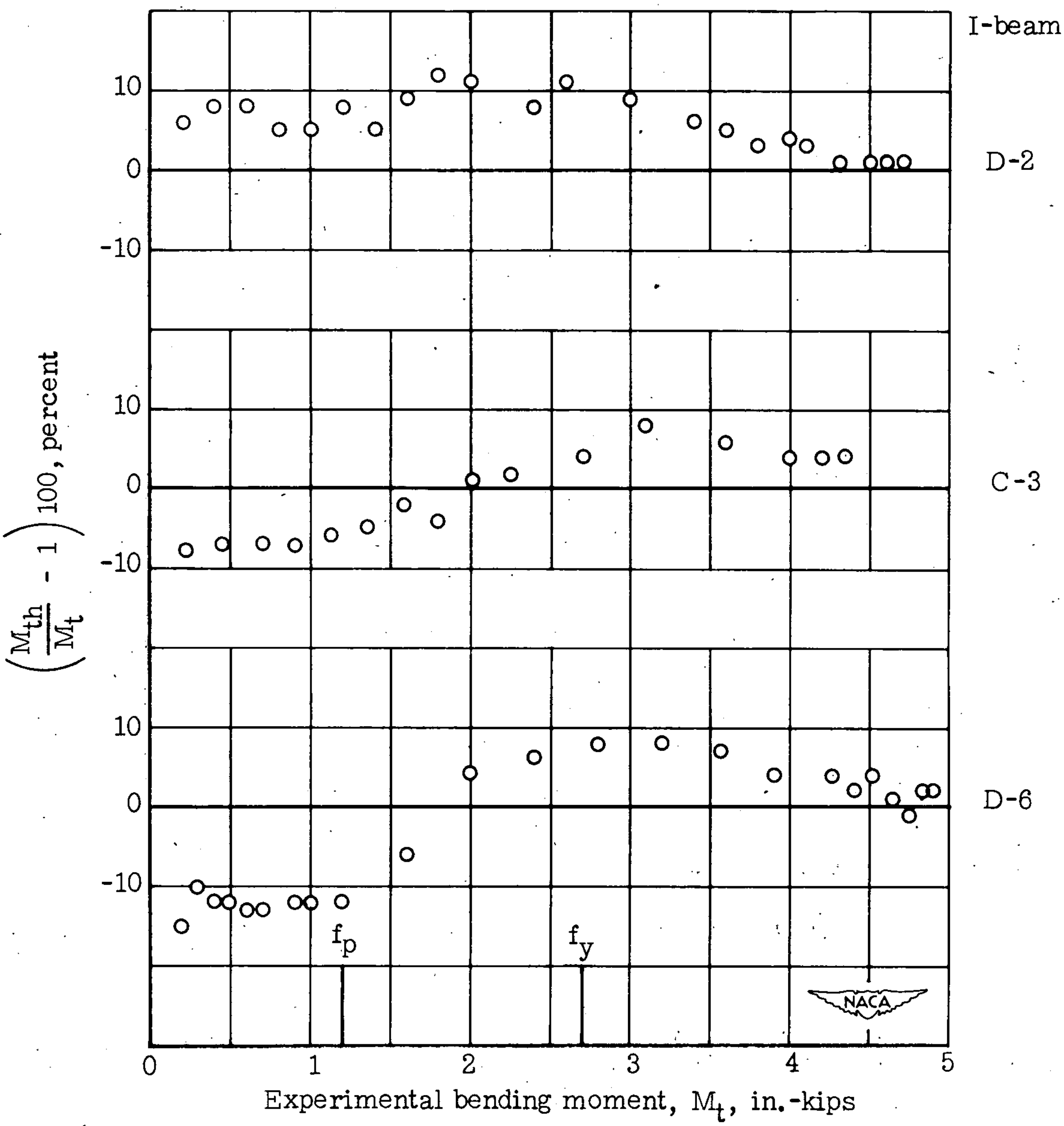

(d) $\theta = 90^{\circ}$.

Figure 24.- Concluded.

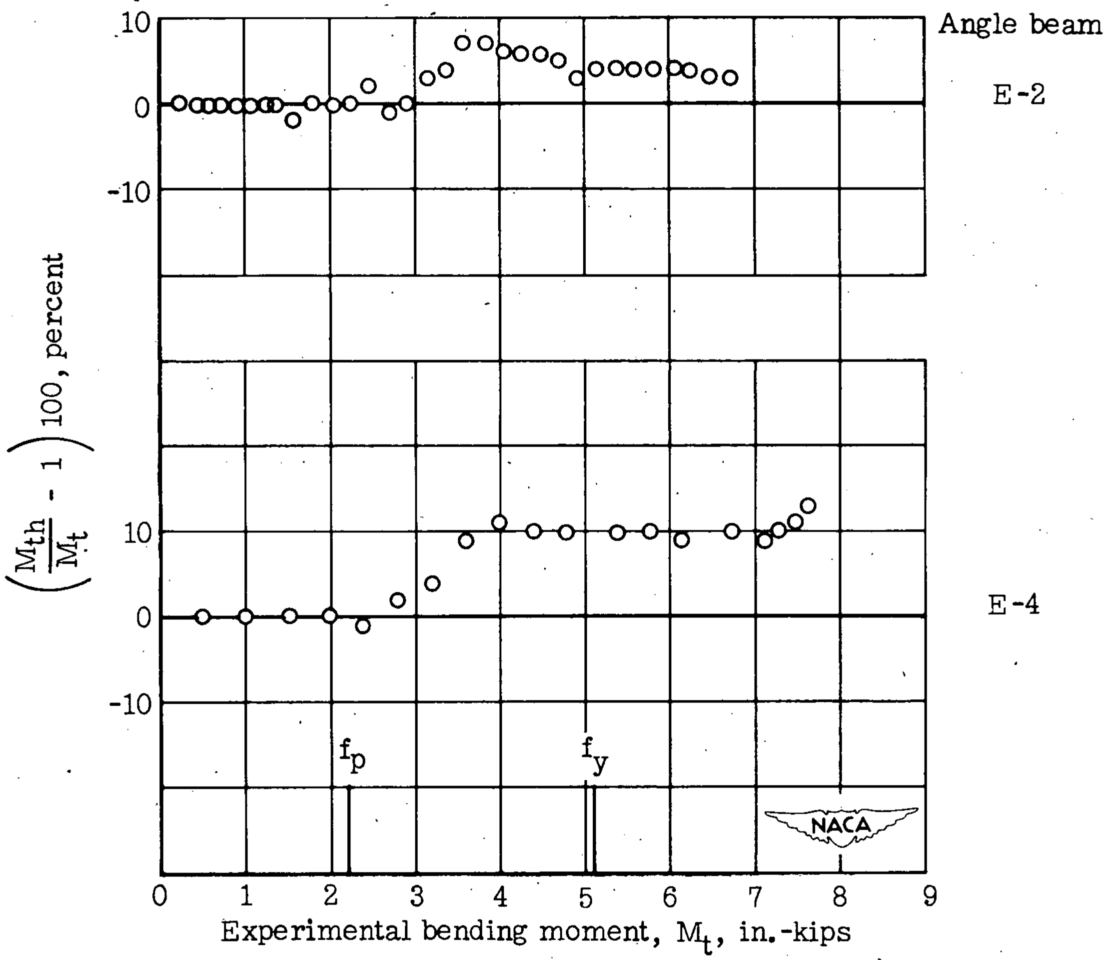

(a) $\theta = 0^{\circ}$.

Figure 25.- Difference between experimental and computed bending moments for angle beams.

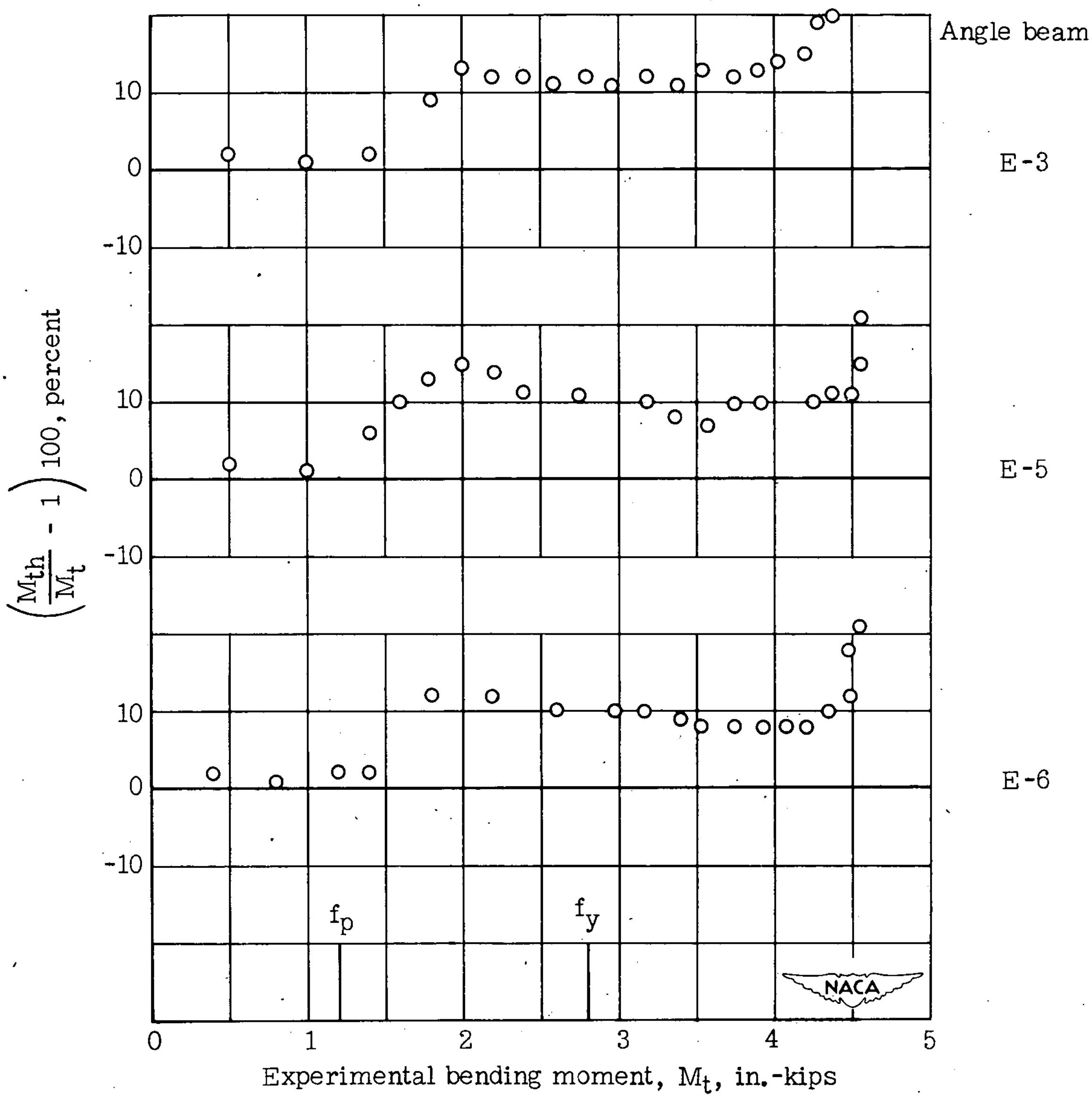

(b) $\theta = 30^{\circ}$.

Figure 25.- Continued.

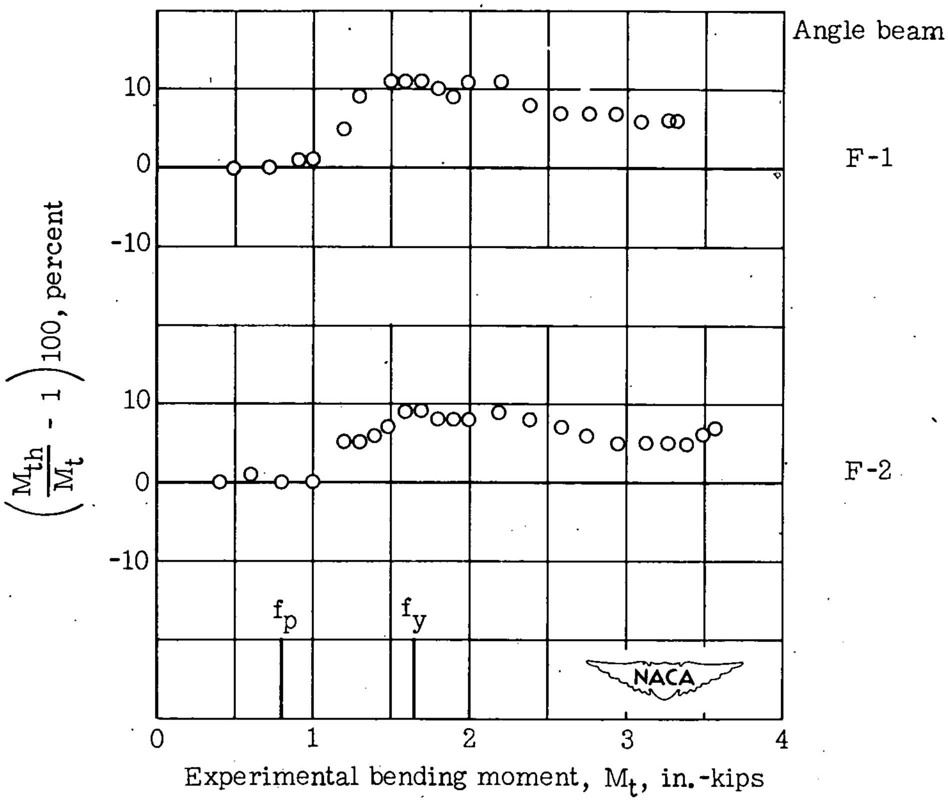

(c) $\theta = 60^{\circ}$.

Figure 25.- Continued.

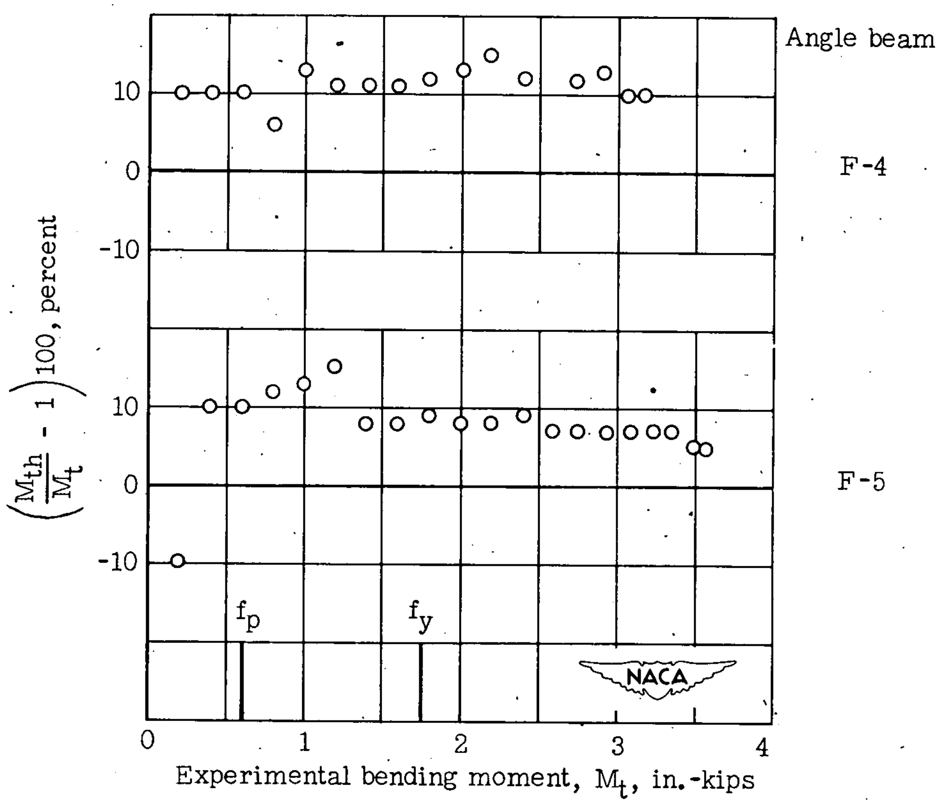

(d) $\theta = 90^{\circ}$.

Figure 25.- Concluded.

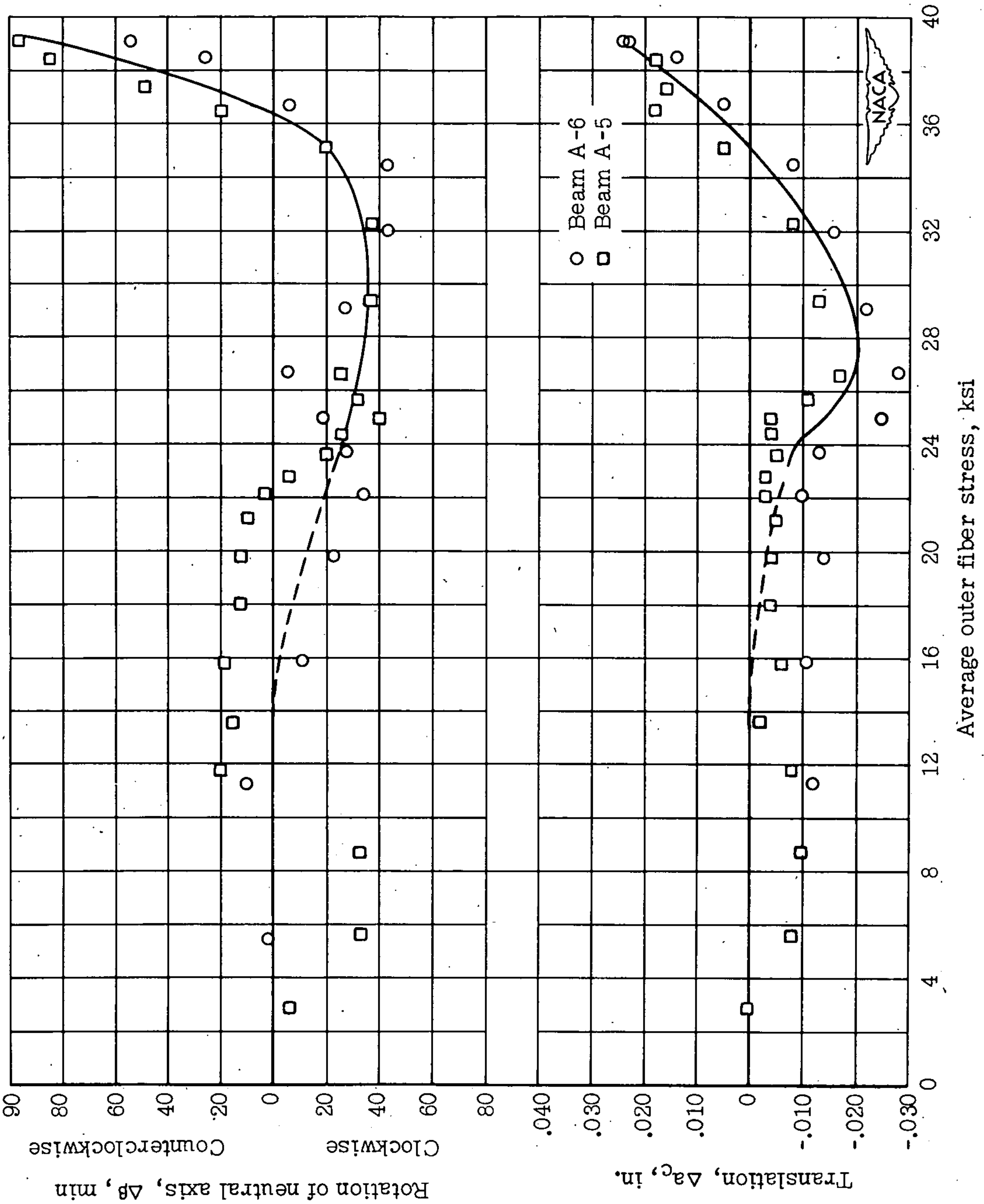

Figure 26.- Rotation and translation of neutral axis. Rectangular beams; $\theta = 30^{\circ}$.